Projecting future fire regimes in semiarid systems of the inland northwestern U.S.: interactions among climate change, vegetation productivity, and fuel dynamics

Jianning Ren[1,1], Erin Hanan[1,1], John T Abatzoglou[2,2], Crystal Kolden[3,3], Christina Tague[4,4], Maureen C Kennedy[5,5], Mingliang Liu[6,6], and Jennifer Adam[7,7]

[1]University of Nevada, Reno
[2]University of California Merced
[3]UC Merced
[4]University of California, Santa Barbara
[5]University of Washington
[6]Unknown
[7]Washington State University

August 8, 2023

Abstract

Fire regimes are influenced by both exogenous drivers (e.g., increases in atmospheric CO2; and climate change) and endogenous drivers (e.g., vegetation and soil/litter moisture), which constrain fuel loads and fuel aridity. Herein, we identified how exogenous and endogenous drivers can interact to affect fuels and fire regimes in a semiarid watershed in the inland northwestern U.S. throughout the 21st century. We used a coupled ecohydrologic and fire regime model to examine how climate change and CO2 scenarios influence fire regimes over space and time. In this semiarid watershed we found that, in the mid-21st century (2040s), the CO2 fertilization effect on vegetation productivity outstripped the effects of climate change-induced fuel decreases, resulting in greater fuel loading and, thus, a net increase in fire size and burn probability; however, by the late-21st century (2070s), climatic warming dominated over CO2 fertilization, thus reducing fuel loading and fire activity. We also found that, under future climate change scenarios, fire regimes will shift progressively from being flammability to fuel-limited, and we identified a metric to quantify this shift: the ratio of the change in fuel loading to the change in its aridity. The threshold value for which this metric indicates a flammability versus fuel-limited regime differed between grasses and woody species but remained stationary over time. Our results suggest that identifying these thresholds in other systems requires narrowing uncertainty in exogenous drivers, such as future precipitation patterns and CO2 effects on vegetation.

Projecting future fire regimes in semiarid systems of the inland northwestern U.S.: interactions among climate change, vegetation productivity, and fuel dynamics

[1,2]Jianning Ren, [2]Erin J. Hanan, [3]John T. Abatzoglou, [3]Crystal A. Kolden, [4]Christina (Naomi) L. Tague, [5]Maureen C. Kennedy, [1]Mingliang Liu, [1]Jennifer C. Adam

[1] Department of Civil & Environmental Engineering, Washington State University, 99163, Pullman, USA

[2] Department of Natural Resources and Environmental Sciences, University of Nevada, Reno, 89501, Reno, USA

[3] Management of Complex Systems, University of California, Merced, 95344, Merced, USA

[4] Bren School of Environmental Science & Management, University of California, Santa Barbara, 93106, Santa Barbara, USA

[5]School of Interdisciplinary Arts and Sciences, Division of Sciences and Mathematics, University of Washington, Tacoma, 98402, Tacoma, USA

Correspondence to:

Jennifer Adam (jcadam@wsu.edu)

Key Points:

- Fire activity in a semiarid ecosystem is projected to increase in the 2040s (i.e., 2031 – 2060) and decrease in the 2070s (i.e., 2061 – 2090).
- While climate change (without CO_2 fertilization) decreases fire activity by reducing fuel load, CO_2 fertilization counteracts this effect to some extent.

- For a given vegetation type, there are temporally stable thresholds—specifically, the ratio of changes in fuel loading to changes in fuel aridity—that determine whether a location is fuel or flammability limited.

Abstract

Fire regimes are influenced by both exogenous drivers (e.g., increases in atmospheric CO_2 and climate change) and endogenous drivers (e.g., vegetation and soil/litter moisture), which constrain fuel loads and fuel aridity. Herein, we identified how exogenous and endogenous drivers can interact to affect fuels and fire regimes in a semiarid watershed in the inland northwestern U.S. throughout the 21st century. We used a coupled ecohydrologic and fire regime model to examine how climate change and CO_2 scenarios influence fire regimes over space and time. In this semiarid watershed we found that, in the mid-21st century (2040s), the CO_2 fertilization effect on vegetation productivity outstripped the effects of climate change-induced fuel decreases, resulting in greater fuel loading and, thus, a net increase in fire size and burn probability; however, by the late-21st century (2070s), climatic warming dominated over CO_2 fertilization, thus reducing fuel loading and fire activity. We also found that, under future climate change scenarios, fire regimes will shift progressively from being flammability to fuel-limited, and we identified a metric to quantify this shift: the ratio of the change in fuel loading to the change in its aridity. The threshold value for which this metric indicates a flammability versus fuel-limited regime differed between grasses and woody species but remained stationary over time. Our results suggest that identifying these thresholds in other systems requires narrowing uncertainty in exogenous drivers, such as future precipitation patterns and CO_2 effects on vegetation.

Plain Language Summary

Many studies have projected increases in wildfire under future climate change. However, in addition to changes in fuel aridity, this also depends on how the fuel loading change in response to warmer temperatures and increasing atmospheric CO_2 concentrations. We used a

coupled ecohydrological and fire model to simulate how wildfire changes in a semiarid watershed of the northwestern U.S. throughout the 21st century. We found that wildfire is projected to increase in the mid-21st century due to increases in fuel loading and fuel aridity. However, wildfire is projected to decrease in the late-21st century due to drought-induced decreases in fuel loading, even when fuels are drier. We demonstrated that future wildfire regimes are dynamic, and we cannot simply extrapolate fire activity from the baseline and 2040s scenarios to the 2070s. Furthermore, we found there was a clear threshold in the ratio of the change in fuel loading to the change in its aridity at which fire regimes shift from being flammability to fuel-limited. Predicting future wildfires will require reducing key uncertainties in future precipitation patterns and our understanding of how CO_2 fertilization affects plant growth.

Key words: fire regimes, climate change, fuel aridity, fuel loading, vegetation, fire regime modeling, fire prediction, semiarid watersheds.

1 Introduction

While frequent low-intensity fires are an important component of many forest ecosystems, e.g., contributing to the regulation of energy, water, and carbon cycling (Flitcroft et al., 2016; Liu et al., 2013), large, stand-replacing wildfires are becoming more common in locations that historically burned at low intensity (Abatzoglou & Williams, 2016; Westerling, 2016; Williams et al., 2019). These fire regime shifts can transform ecosystem dynamics and structure, increase air and water pollution, cause flood and landslide hazards, and threaten human property and lives (Abatzoglou et al., 2014; Smith et al., 2016). Climate change is a major factor pushing fire regimes in flammability-limited forested systems outside their historical range of variability (Abatzoglou & Williams, 2016). Thus, mitigating future fire hazard requires understanding how climate change and wildfire interact at the scales where management actions

are implemented. However, this is challenging at fine scales because climate-wildfire interactions can vary with local environmental conditions, including topography and vegetation cover (Hanan et al., 2021; Littell et al., 2018; Pausas & Paula, 2012).

While climate change is playing an essential role in facilitating large fires in the western U.S. (Abatzoglou & Williams, 2016), the effects of climate change are location-dependent. For example, climate change (i.e., warming) can increase the frequency, duration, and intensity of drought, which can in turn increase fuel aridity and fire hazard (Abatzoglou & Kolden, 2013). This is especially true in mesic landscapes where wildfire regimes are flammability-limited. In more arid locations, on the other hand, climate change may ultimately decrease wildfire hazard by reducing net primary productivity (NPP) and, therefore, fuel loads (Hanan et al., 2021; Littell et al., 2016, 2018). Thus, the effects of climate change on future fire regimes depends in large part on how vegetation (and fuels) respond.

Understanding how climate change influences vegetation, fuel aridity, and fuel loading is further complicated by the role of rising atmospheric CO_2 concentrations, which can modify plant (and therefore fuel) responses to drought (Becklin et al., 2017; Warren et al., 2011). For example, increasing CO_2 concentrations can increase plant productivity by increasing photosynthetic and water-use efficiency, thereby partially offsetting the suppressive effects of drought (Becklin et al., 2017; Lewis et al., 2009; Sullivan et al., 2020). Because rising CO_2 concentrations and warming influence vegetation, fuel loading, and fuel moisture in opposite ways, it is important to disentangle which drivers dominate in different locations.

Many recent studies have focused on understanding how climate, ecosystem structure, and fuel conditions interact to drive wildfire regimes at different scales (Abatzoglou & Kolden, 2013; Halofsky et al., 2020; Hicke et al., 2012; McCarley et al., 2017; Williams et al., 2019).

However, many of these observational studies are limited in their ability to isolate specific drivers or project into the future (Hicke et al., 2012; McCarley et al., 2017). Alternatively, empirical models have been used to predict future fire regimes (e.g., Abatzoglou et al., 2019; Bradstock, 2010; Littell et al., 2018; Liu et al., 2013; McKenzie et al., 2004). However, empirical models do not consider dynamic vegetation and changes in fuel loading that occur under climate change (Pausas & Paula, 2012). Process-based models are a key tool for complimenting field-based and empirical modeling studies; they can bridge spatial and temporal scales while also accounting for feedbacks among climate change, rising CO_2, vegetation productivity, and fire. They also enable researchers to manipulate drivers to isolate their individual and combined effects (Hanan et al., 2021).

In this study, we addressed the overarching question: **What role does vegetation play in influencing the effects of climate change on fire regimes in a semiarid watershed?** We applied the coupled ecohydrological, fire regime modeling platform RHESSys-WMFire (Bart et al., 2020; Kennedy et al., 2017; Tague & Band, 2004) in a semiarid watershed in the U.S. Inland Northwest. We used a range of possible future scenarios to assess how climate change and increasing atmospheric CO_2 interact to influence vegetation and, thus, the roles of fuel loading and fuel aridity in determining future fire regimes. Specifically, we addressed the following questions:

(1) What are the relative and opposing roles of two key *exogenous* drivers in driving fire regimes: climate change (warming and changes in precipitation) and increasing CO_2 (*Figure 1*)?

(2) What are the relative and opposing roles of two key *endogenous* drivers in driving fire regimes: fuel load and fuel aridity (*Figure 1*)?

Climate change and increasing CO_2 can either compete or compound one another to influence fuel aridity, fuel loading, and resultant fire regimes. The extent to which a particular ecosystem is affected by either mechanism depends on whether or not fire is limited by fuel (biomass available for burning) or flammability (environmental conditions that enable the fuel to burn, which are partially controlled by climate, Abatzoglou et al., 2019; Littell et al., 2018; Werf et al., 2008). We hypothesize that climate change can affect fuel loading and fuel aridity through changes in vegetation productivity, evapotranspiration (ET), and litter decomposition. At finer scales, historical aridity gradients across the watershed (PET/P) also play an important role in determining the spatial distribution of how fire regimes respond to climate change (Hanan et al., 2021). Thus, it is essential to account for these biophysical and biogeochemical processes in projections of future fire regimes in order to improve our understanding of how fire regimes are changing in semiarid landscapes and support policy and other decision-making processes at management-relevant scales.

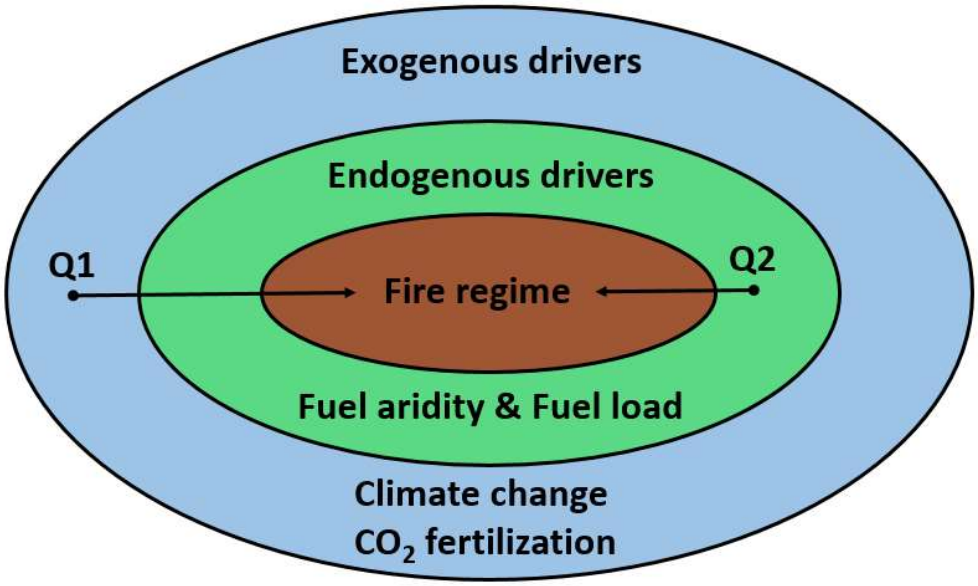

Figure 1. Exogenous (external) and endogenous (internal) drivers of fire regimes. Question 1 (Q1) focuses on the role of exogenous drivers while Question 2 (Q2) focuses on endogenous drivers.

2 Methods

2.1 Study area

Trail Creek is a 167-km^2 sub-catchment of the Big Wood River Basin located in Blaine County, Idaho, between the Salmon-Challis National Forest and Sawtooth National Forest (43.44N, 114.19W; *Figure 2*). The mean annual precipitation in the area is around 980 mm, of which 60% is snow (Frenzel, 1989). Trail Creek is characterized by cold, wet winters and warm, dry summers. Elevations range from 1760 to 3478 m, and there is a vegetation and aridity gradient following changes in elevation. To describe the spatial variation of atmospheric aridity (which is different from fuel aridity), we use the ratio of multi-year average annual potential evapotranspiration (PET) to multi-year average annual precipitation (P) as an index. We define areas with PET/P>2 as water-limited, PET/P<0.8 as energy-limited, and PET/P between 0.8 and 2 as balanced (McVicar et al., 2012). As *Figure 2*depicts, lower to middle elevation slopes are

water-limited and covered by sagebrush (*Artemisia tridentata ssp.*), mixed riparian species, and grasslands; middle to higher elevation areas are water-energy balanced and are covered by Douglas fir (*Pseudotsuga menziesii*), lodgepole pine (*Pinus contorta varlatifolia*), subalpine fir (*Abies lasiocarpa*), and mixed shrub and herbaceous vegetation (Buhidar, 2001). Soils in Trail Creek are mainly coarse, permeable alluvium (Smith, 1960). No wildfires have occurred in the last 40 years. The soils, vegetation and topography, however, are comparable to several sub-catchments on the western side of the Big Wood River Basin, which were burned in the 2013 Beaver Creek Fire (total 45,036 ha burnt area, Skinner, 2013).

Table 1. Fire regime groups and corresponding characteristics (Rollins, 2009).

Fire Regime Group	Characteristics
Fire Regime Group I	<= 35-year fire return interval, low and mixed severity
Fire Regime Group II	<= 35-year fire return interval, replacement severity
Fire Regime Group III	35 to 200-year fire return interval, low and mixed severity
Fire Regime Group IV	> 200-year fire return interval, any severity

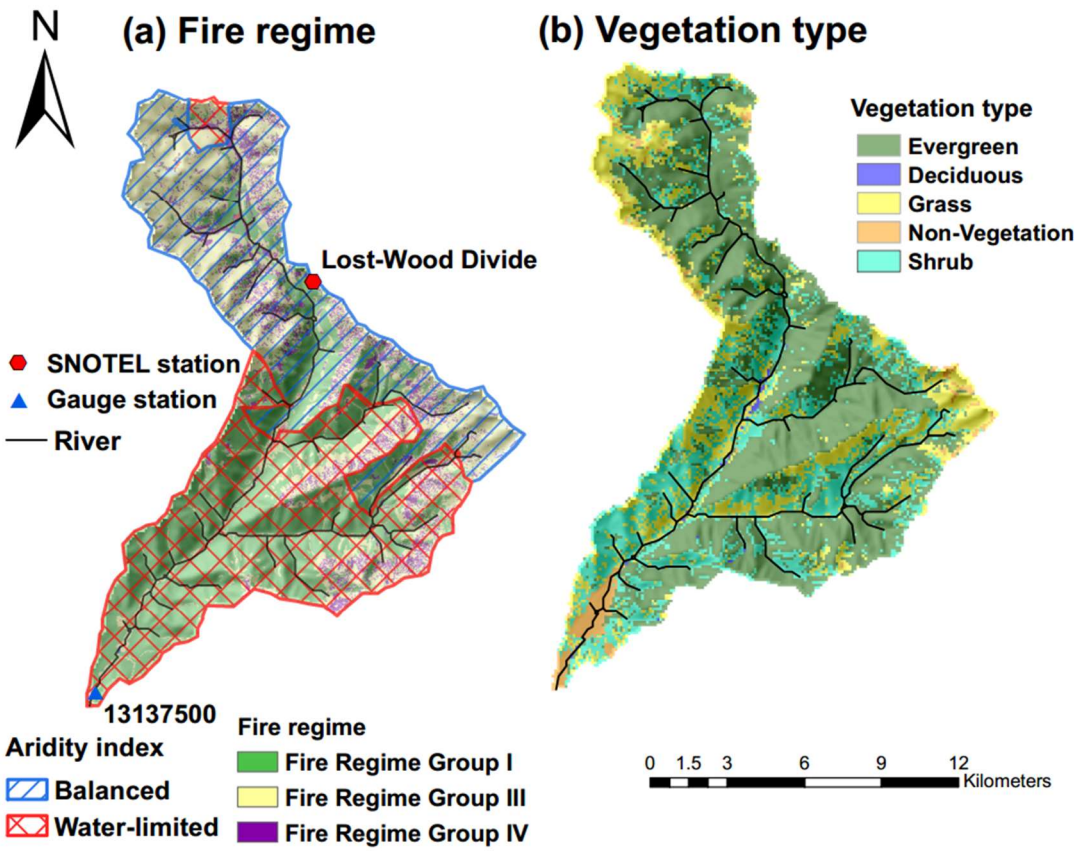

157

158 *Figure 2. Study site – Trail Creek. (a) fire regime from LANDFIRE data (* Rollins, 2009*; Table*
159 *1); the gridded areas show different long-term aridity indices; (b) land cover overlapped with*
160 *topography (*elevations range from 1760 to 3478 m).
161
162 The aridity index generally correlates with the fire regime classifications from
163 LANDFIRE, which are based on vegetation cover, ecological and vegetation simulation, and
164 successional modeling (Fig. 2; Rollins, 2009). In the lower part of the basin, the mean
165 LANDFIRE fire return interval (FRI) is short (i.e., 35 years) and fires are generally low or mixed
166 severity. This is a fuel-limited fire regime (the fuels are dry enough to burn in most years, but
167 there is rarely enough fuel to carry fire). The upper part of the basin, on the other hand, has a
168 long mean FRI (i.e., 200 years) and typically burns at high severity. This is a flammability-
169 limited fire regime (there is enough fuel present, but fuels are generally too moist to burn;
170 LANDFIRE, Rollins 2009, *Figure 2*, *Table 1*). The central part of the basin is a transitional zone,

with some fuel-limited patches located in relative mesic areas, and some flammability-limited patches located in more water-limited areas. Within the northern part of the basin there is also a small water-limited area due to slightly lower precipitation.

2.2 Model description

We used the coupled ecohydrologic-fire regime modeling platform RHESSys-WMFire (Kennedy et al., 2017; Bart et al., 2020) to model fire and vegetation responses under a range of climate and CO_2 scenarios. The Regional Hydro-ecologic Simulation System (RHESSys, Tague & Band, 2004) is a mechanistic model designed to simulate the effects of climate and land use change on ecosystem carbon (C) and nitrogen (N) cycling and hydrology. RHESSys fully couples hydrology (streamflow, ET, soil moisture), C (photosynthesis, respiration, net primary productivity=NPP, mortality) and N fluxes (mineralization, nitrification, denitrification, plant uptake, and leaching) at a hierarchy of scales (e.g., patch, zone, sub-basin, basin). Photosynthesis is calculated based on the Farquhar model, which is a function of nitrogen, radiation, stomatal conductance, atmospheric pressure, atmospheric CO_2 concentration, and daily average temperature (Farquhar & von Caemmerer, 1982). Higher atmospheric CO_2 concentrations can increase photosynthesis rates (i.e., CO_2 fertilization). Stomatal conductance is based on the Jarvis model of stratum conductance (Jarvis, 1976), which accounts for the effects of light, atmospheric CO_2 concentration, leaf water potential, and vapor pressure deficit (Running & Coughlan, 1988; Tague & Band, 2004). Recent empirical studies have shown that higher CO_2 concentration can increase plant water use efficiency but with large uncertainties (Becklin et al., 2017; Duursma et al., 2014). Therefore, we did not include the effect of CO_2 augmentation on stomatal conductance and only considered the CO_2 fertilization effect on photosynthesis. Litter decomposition models are based on the method developed by Thornton, (1998), which is related

to the C:N ratio and potential decay rate. The potential decay rate is limited by soil moisture, temperature, and nitrogen, and a higher temperature may cause a higher decay rate. RHESSys has been widely tested and applied in many mountainous watersheds (Garcia & Tague, 2015; Hanan et al., 2017, 2018, 2021; Lin et al., 2019; Ren et al., 2021; Son & Tague, 2019). A more detailed description of the RHESSys model can be found in Tague & Band, (2004).

RHESSys-WMFire couples RHESSys with a model for fire spread (WMFire, Kennedy et al., 2017) and a model for fire effects (Bart et al., 2020), which capture fuel and climate controls on fire spread and severity. RHESSys-WMFire computes key processes at a daily time-step and partitions the landscape into patches (the smallest spatial unit, typically 30-120 m). The model therefore accounts for spatial differences in energy and precipitation conditions on soil moisture, evapotranspiration, vegetation growth, and fire dynamics. Notably the model accounts for the lateral downslope redistribution of water. WMFire is a stochastic model that requires several replicate simulations (200 in the current study) to attain a representative result (Kennedy, 2019). Additional details on the model framework and parameter calibration are provided in supplementary material text S1 and S2.

2.3 Input data

2.3.1 Selection of GCM models (storylines) and CO_2 data

Because RHESSys-WMFire is computationally intensive, we selected four General Circulation Models (GCM) based on changes in climate variables that are most related to fire activity between the historical (1971 – 2000) and future (2040 – 2069) periods. For selecting GCM models, we used three variables: 1) a measure of annual water deficit (DEF), calculated as potential evapotranspiration (PET) minus actual evapotranspiration (AET), 2) a measure of annual plant available moisture (i.e., AET), and 3) 100-hour dead fuel moisture (FM100) in

summer, defined as a biomass volume that takes 100 hours to lose or gain 2/3 of the difference between the dead fuel itself and the surrounding atmosphere. Note that for the purpose of GCM selection, PET and AET was estimated at monthly time scales (Abatzoglou & Rupp, 2017). The first variable (DEF) is a proxy of changes in vegetation moisture stress that enable flammability and is most important in modulating burned area in flammability-limited forests. The second variable (AET) is a proxy for potential changes in plant productivity and fuel accumulation and is therefore more important for modulating fire occurrence in fuel-limited environments. The differences in standard deviation (SD) of PET and AET between the future and the historical climate is also important because climate variability can exacerbate or temper fire return intervals. FM100 is calculated based on the National Fire Danger Rating System using climate data from GCMs (Cohen & Deeming, 2006).

We started with 20 GCMs from the Coupled Model Inter-comparison Project 5 (CMIP5; Taylor et al., 2012) that have been statistically downscaled across the contiguous U.S. using the Multivariate Adaptive Constructed Analogs (MACA, Abatzoglou & Brown, 2012) with 1/24 degree resolution (~4-km) covering the time period from 1950 to 2100. Then, we used six metrics based on the assessment criteria described above to select future climate scenarios: the change in mean AET and DEF (i.e., 2040 – 2069 mean vs. 1971 – 2000 mean); the standard deviation of monthly AET and DEF; and the number of days per year where FM100 in the future (i.e. 2040-2069) is less than the 3rd percentile value for the historical period (i.e. 1971 – 2000), and the 10th percentile. Based on the ranking shown in Figure S1, we selected four models to cover the range of all 20 GCMs, as well as a model representing the mean behavior (IPSL-CM5A-LR, **MultiMean**): one with a large increase in aridity that may promote drought (CSIRO-Mk3-6-0, **ProDrought**), one that promotes increased productivity but limits fire (GFDL-

ESM2G, **ProVeg**), and one with a significant fluctuation of fire-related metrics (INMCM4, **ProFire**). For forcing RHESSys-WMFire, we select representative concentration pathway (RCP) 8.5 due to its close agreement with historical total cumulative CO_2 emissions during the historical time period (Meinshausen et al., 2011; Schwalm et al., 2020).

Table 2. Lists of four selected GCM model based on fire-related characteristics.

GCM #	Storyline Name	Model Name	Characteristics
1	ProDrought	CSIRO-Mk3-6-0	A large increase in summer aridity that may promote drought
2	ProVeg	GFDL-ESM2G	Promotes increased productivity and limits fire
3	ProFire	INMCM4	A significant increase in fire-related metrics (FM100)
4	MultiMean	IPSL-CM5A-LR	Close to the multi-model mean

To evaluate the effect of rising CO_2 concentrations, we used observed and projected CO_2 concentrations from 1900 to 2099 produced by Meinshausen et al., (2011) based on the Intergovernmental Panel on Climate Change Fourth Assessment Report (IPCC AR4). For the "with CO_2 fertilization effect", we use transient CO_2 concentration from AR4; and for the "without CO_2 fertilization effect", we use constant CO_2 concentration, i.e. 353 ppm-the concentration in year 1990

2.3.2 Model calibration and initialization

For soil parameter calibration, we used daily, high-resolution (1/24 degree or ~ 4 km) gridded meteorological data from GridMET (*Table 3* A), including minimum and maximum temperatures, precipitation, relative humidity, shortwave radiation, and wind speed covering the

time period from 1895 to 2017. We used raw gridMET data from 1980 to 2017 (Abatzoglou, 2013) to reconstruct the historical record from 1895 to 1979 (Hanan et al., 2021) based on Parameter-elevation Relationships on Independent Slopes Model data (PRISM, Daly et al., 1994) and the European Center for Medium-Range Weather Forecast (ECMWF) reanalysis data (Simmons & Gibson, 2000).

After model calibration, we initialized vegetation and soil C and N pools using a target-driven spin-up approach (Hanan et al., 2018). During the vegetation initialization period, we used the same observed climate data from model calibration, but with the anthropogenic climate change signal removed (*Table 3* B) per Hanan et al., (2021). We ran the model for 300 years with this modified climate data and with the fire model "on" to initialize the landscape vegetation. From this we obtained the pre-industrial and pre-suppression condition as a starting point for running different climate change scenarios. The vegetation initialization was conducted once for all scenarios, i.e. they have same initial state of vegetation, litter, and soil C & N storage.

Table 3. Climate forcing data, atmospheric CO_2 concentration, and their usage for this study.

Label	Forcing data name	Data period	Data source	Manipulations	Purpose
A	Observed climate data	1895 - 2017	gridMET, ECMWF and PRISM	gridMET reconstructed with PRISM	Calibration
B	Observed climate data with anthropogenic signal removed	1895 - 2017	gridMET, ECMWF and PRISM	Use ensemble of 20 MACA downscaled GCMs to remove the historical climate signal from observed data	Vegetation initialization (looped the data over 300 years)

C	Baseline climate	1950 - 2005	CMIP5	MACA downscaled	Future fire scenarios spin-up and fire assessment
D	RCP8.5 climate data	2006 - 2099	CMIP5	MACA downscaled	
E	Transient CO_2 concentrations	1900-2099	IPCC AR4	NA	

271

272 2.3.3 Other biophysical and land cover data

273 We aggregated a 10-m resolution digital elevation model (DEM) from the US Geologic
274 Survey National Elevation Database to 100-m resolution (USGS, NED 2016) to generate the
275 topographic properties and watershed structure of Trail Creek, which include elevation, slope,
276 aspect, patches, sub-basins, and basin boundaries. In total, we delineated 72 sub-basins and
277 16,705 patches. We use the National Land Cover Database (NLCD 2016, Dewitz, 2019) to
278 classify five vegetation types. Of these, 49.6% were evergreen, 24.9% were shrub, 22.0% were
279 grass, 0.3% were deciduous, and 3.1% were not vegetated. Soil type was assigned using a spatial
280 continuous probability soil map (POLARIS) created by Chaney et al. (2016).

281 2.4 Modeling scenarios and climate forcing

282 We conducted model simulations using RHESSys-WMFire over three major timeframes
283 for each GCM, both with and without CO_2 fertilization: baseline, 2040s, and 2070s. The 2040s
284 and 2070s timeframes were simulated with the RCP8.5 (Meinshausen et al., 2011). For each
285 timeframe there was a 55-year spin-up and a 30-year assessment time period (*Figure 3*) for a
286 total 85-year simulation with the fire model turned on. Each spin-up period was initialized with
287 the same initial conditions generated in the vegetation initialization described above.

For the baseline scenario, we first ran the model for 55 years using historical GCM forcing inputs from each of the 4 chosen GCMs (1950-2005; *Table 3*). We then repeated the climate data over the years 1950-1964 and 1991-2005 to generate the 30-year baseline assessment period. Climate change effects were assessed against the patterns seen in the baseline time period.

For the future scenarios, we simulated a 55-year spin-up period using each of the 4 GCMs and starting with the same vegetation initialization described above. We then repeated the last 15 years of the climate data and combined it with the next 15 years to produce the assessment period. For example, for the 2040s simulation we spun the model up for 55 years using climate data from 1991-2045, then simulated an additional 30-year assessment period using climate data from 2031-2060. For the 2070s simulation we spun the model up for 55 years using climate data from 2021-2075, then simulated an additional 30-year assessment period using climate data from 2061-2090. All simulations were repeated with and without CO_2 fertilization for each of the 4 GCMs.

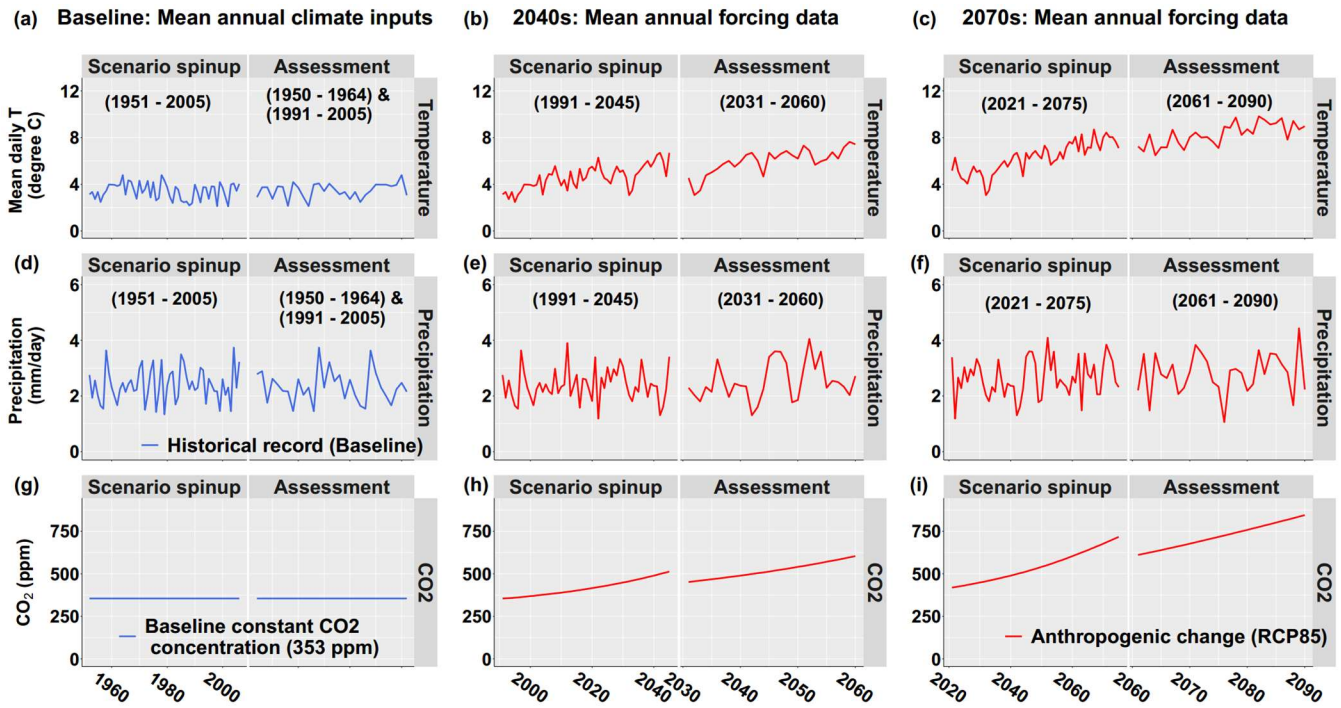

Figure 3. Future fire simulation scenarios using the ProDrought GCM as an example. b, e, and h show the assessment of the 2040s (2031 to 2060); c, f, and i show the assessment of 2070s (2061 – 2090); a, d, and g are for baseline scenarios. There are three simulation periods: the vegetation initialization period (not shown), the scenario spin-up period, and the assessment period. For the scenario spin-up period, there were two different climate inputs: baseline and RCP8.5; and two different CO_2 fertilization scenarios (with and without). We used the historical output from individual GCMs as a baseline for calculating future climate change effects. For the scenario spin-up period, the baseline scenario used historical data from 1951 to 2005. For the *assessment period (30 years), the baseline scenario used data that concatenated the first 15 years of the historical record (1950 -1964) to its last 15 years records (1991 -2005). We considered the future climate and CO_2 fertilization scenarios in isolation and together to build different landscape fuel conditions for the subsequent assessment periods. For the CO_2 fertilization effect, we used transient CO_2 concentrations from IPCC as the model input; for the no CO_2 fertilization scenarios, we used a constant CO_2 concentration (i.e., 353 ppm). For the assessment period (30 years), we use the spun-up fuel conditions as initial conditions and ran the fire model to assess the relative contribution of different factors in driving fire regimes.*

Table 4. Summary of model simulation scenarios. "Climate change" refers to the climate change effect with no CO_2 fertilization (using constant CO_2 concentration - 353 ppm as the model input). "Climate change and increasing CO_2" refers to their combined effects (using both RCP8.5 climate data and transient CO_2 concentrations as inputs. Meinshausen et al., 2011).

ID	Scenarios	Representing period	Forcing data	
			Climate data	CO_2 data
1	Baseline	Baseline (30 years)	Historical (Table 3 C)	353 ppm
2	Climate change (2040s)	2040s (2031-2060)	RCP8.5 (Table 3 D)	353 ppm
3	Climate change and increasing CO_2 (2040s)	2040s (2031-2060)	RCP 8.5 (Table 3 D)	transient CO_2 (Table 3 E)
4	Climate change (2070s)	2070s (2061-2090)	RCP8.5 (Table 3 D)	353 ppm
5	Climate change and increasing CO_2 (2070s)	2070s (2061-2090)	RCP 8.5 (Table 3 D)	transient CO_2 (Table 3 E)

For evaluating the changes in fire regimes, we only analyzed outputs for the 30-year assessment period. We calculated 4 main fire characteristics for each of the 200 independent Monte Carlo replicates for each scenario: mean number of patches burned per fire, 95th percentile fire size in 30 years' assessment period, annual area burned (mean number of patches burned each year), and number of fire starts (fires that surpass 30 burned patches in 30 years' assessment period). We then compared distributions of these variables among the model scenarios.

We also considered patch-level summaries of burn probability (P_{burn}), fuel aridity, and fuel loading. For each patch, the burn probability (P_{burn}) was calculated as:

$$p_{burn} = \frac{number\ of\ times\ burned\ across\ all\ simulations}{number\ of\ simulation\ years * number\ of\ simulations} \quad \text{Equation 1}$$

Fuel aridity is calculated by WMFire as relative deficit and was calculated monthly as:

$$Fuel\ aridity = 1 - ET/PET \quad \text{Equation 2}$$

We calculated patch-level mean burn probability, fuel loading, and fuel aridity to understand the relationships among these variables in the different model scenarios.

3 Results

In the following descriptions we use "overall effect" to represent both the climate change and CO_2 fertilization effects on fire activity, while "climate change effect" represents the climate change effects without CO_2 fertilization.

3.1 Effects of climate change and CO_2 fertilization on fire starts and size

During the 2040s assessment period, the **climate change effect** decreased fire size and activity relative to baseline (*Figure 4*). In contrast, the **overall effect** increased or only slightly decreased fire activity and fire size (*Figure 4* a). These patterns correspond to climate change and CO_2 effects on fuel and vegetation. Climate change alone decreased overall fine fuel loading through increases to soil respiration (*Figure S5*), whereas CO_2 fertilization increased fire activity by enhancing vegetation productivity and thus fuel loading (*Figure S6*).

Fire responses differed among GCM storylines. When considering the climate change effect, the ProDrought storyline exhibited the greatest decreases in fire activity and the ProVeg storyline the smallest decrease (*Figure 4*). This occurred because the ProDrought storyline had the largest decrease in fuel loading, which outstripped the effects of increasing fuel aridity (*Figure S2 and Figure S3*). When considering the overall effect (climate change and CO_2), the ProVeg storyline predicted the largest increase in fire size and AAB with no noticeable increase in the number of fire starts (fire that burned more than 30 patches). This occurred because the storyline promoted productivity and, therefore, increases in fuel loading (*Figure S2 and Figure S4*). The MultiMean storyline also predicted an increase in fire size for the overall effect but the

increase was smaller in magnitude than ProVeg. ProFire and MultiMean predicted the most significant increases in the number of fire starts for the overall effect, but differed in their fire size responses (*Figure 4c*).

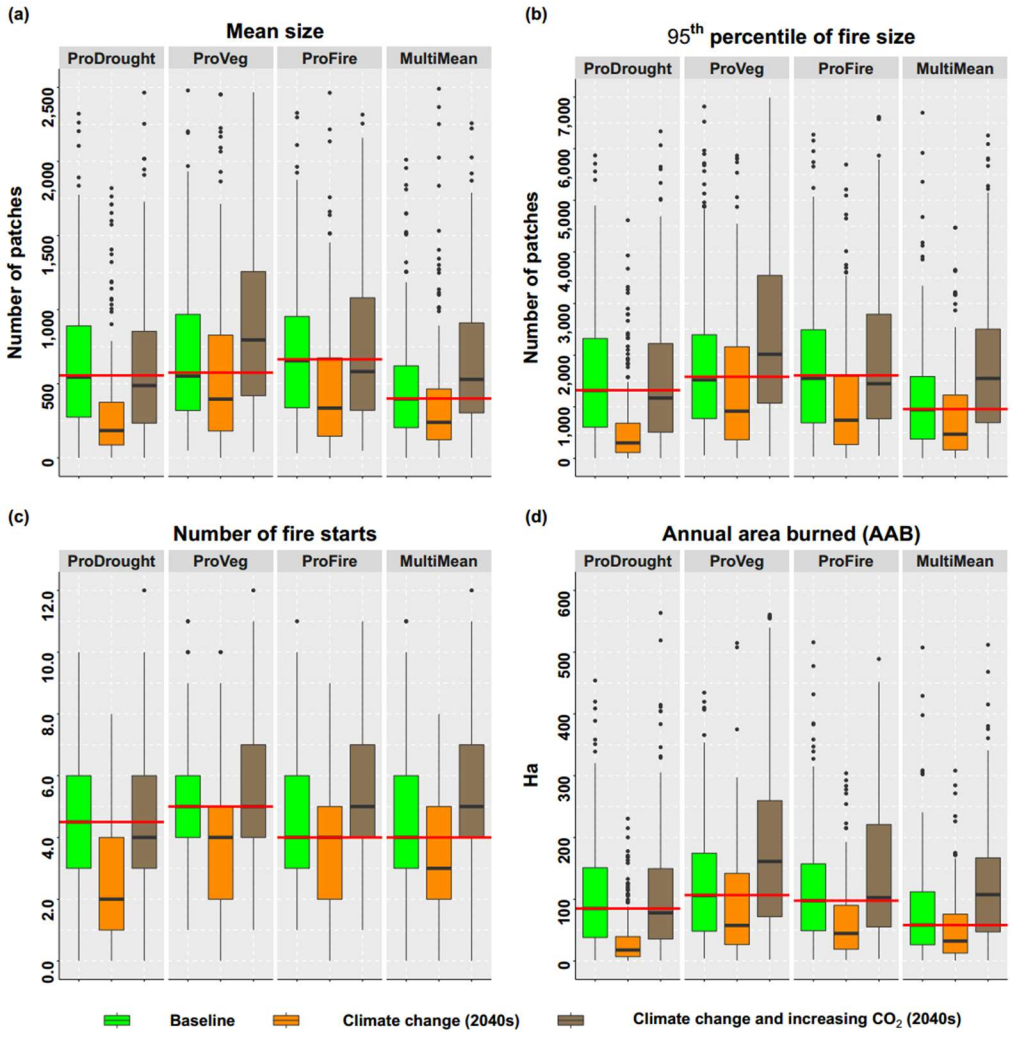

Figure 4. Box plot of projected fire characteristics in 2040s under each climate change and increasing atmospheric CO_2 storyline for the assessment period: (a) mean fire size, (b) 95th percentile fire size, (c) number of fire starts (fires that burned more than 30 patches), and (d) annual area burned. Red lines represent the median value for the baseline scenario. Box plots show medians, 25th and 75th percentiles and 95% confidence intervals. "Climate change (2040s)" refers to the climate change effect without CO_2 fertilization, and "climate change and increasing CO_2 (2040s)" refers to the overall effect. All four fire characteristics were calculated first within each independent simulation replicate (there were 200 simulation replicates for each scenario). Then their distribution across 200 simulations is shown for each scenario.

376 Fire activity had a non-monotonic response to exogenous drivers over the 21st century
377 (i.e., in the 2070s; *Figure 5*). When only considering climate change (for all four GCM
378 storylines), there was a dramatic decrease in all fire metrics in the 2070s compared to the
379 historical scenario, consistent with the simulated decrease for the 2040s. The effect of CO_2
380 fertilization, however, differed between the two timeframes. The overall effect of climate change
381 and CO_2 fertilization was predicted to increase fire activity in the 2040s, but either did not
382 change or decreased predicted fire in the 2070s (*Figure 5*). Warming increased aridity and
383 reduced vegetation productivity (*Figure 8 b&d*), which reduced fuel accumulation. It also
384 increased decomposition rates, which further reduced fuel loading (*Figure S6 and Figure S9*).
385 Faster decomposition of litter and reduced vegetation productivity are the dominate driver than
386 fire-caused fuel combustion in reducing fuel loading. CO_2 fertilization however, increased fuel
387 loading by enhancing vegetation productivity (*Figure S8*), which counteracted warming-induced
388 decreases in fuel loading in 2040s. However, by the 2070s, climate change-driven decreases in
389 fuel loading outstripped any compensatory effects of CO_2 fertilization (*Figure S2 Figure S6*).
390 This led to an overall decrease in fire activity from the 2040s to the 2070s (e.g., *Figure 5a*).

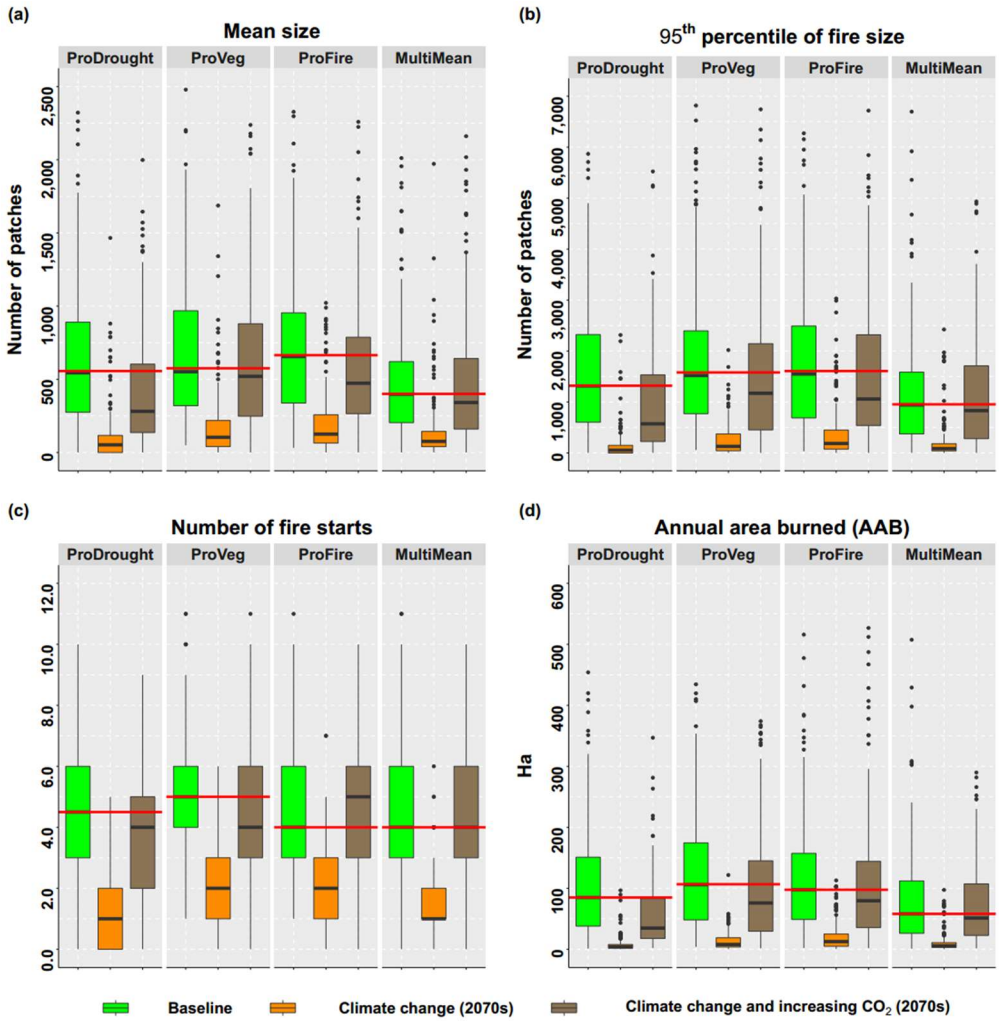

Figure 5. Same as Figure 4, but for the period of 2070s

3.2 Effects of exogenous and endogenous drivers on burn probability (P_{burn})

Fuel conditions varied among vegetation cover types (*Figure 6*). For example, region A (grass-dominated) was very fuel-limited (fuel load < 0.3 kg/m^2, *Figure S10* and *Figure 6 b*) and had a broader range of fuel aridity conditions; region B (shrub-dominated) was fuel-limited (fuel load < 0.5 kg/m^2, *Figure S10* and *Figure 6 b*) and very arid (fuel aridity > 0.6); and region C (evergreen forest) was fuel abundant (fuel load > 0.4 kg/m^2) and relatively humid (0.5 < fuel aridity < 0.85, *Figure S10* and *Figure 6 b*).

In the 2040s, climate change reduced $\mathbf{P_{burn}}$ **(Equation 1)** across the watershed by reducing fuel loading. However, increasing CO_2 tempered that effect, and in many locations even changed its direction (except for in region B, which is shrub-dominated). The counteracting effects of climate change and CO_2 fertilization depended on location and vegetation cover type. Region B (shrub-dominated) had the largest decreases in $\mathbf{P_{burn}}$ due to climate change (except under the ProVeg storyline). This occurred because warming reduced shrub productivity (*Figure 2* & *Figure 8* d) and enhanced litter decomposition, which synergistically reduced fuel loading (*Figure S2*).

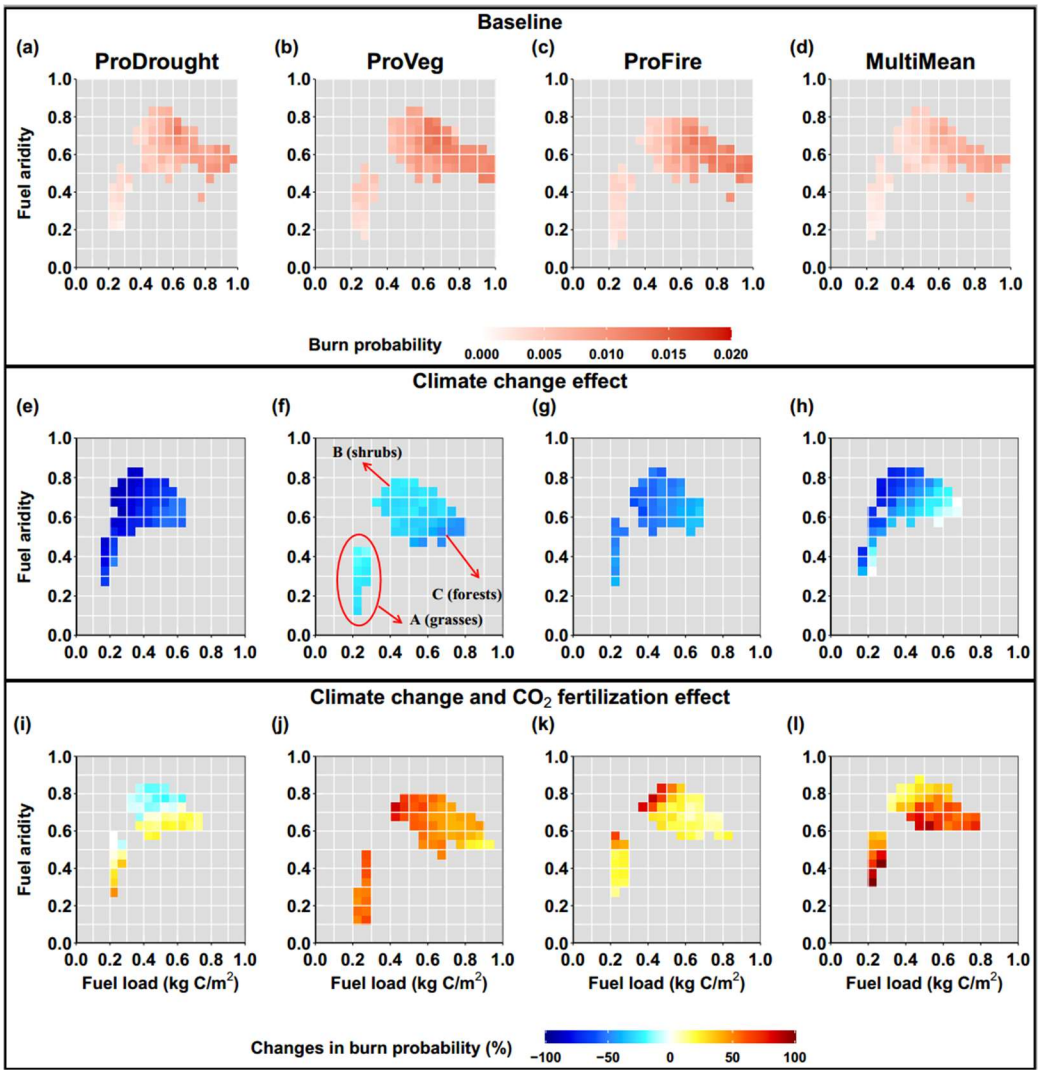

Figure 6. Relationships among fuel load (i.e., litter carbon), fuel aridity, and percent changes in burn probability (relative to the baseline scenario) under various climate change and atmospheric CO_2 fertilization scenarios in the 2040s. Panels (a), (b), (c), (d) show the distribution of burn probability against fuel load and fuel aridity with the baseline scenario as the reference. Other panels show bivariate effects of fuel load and fuel aridity on percentage changes in burn probability (climate change scenario minus baseline scenario). Data are binned with 0.05 window length for both fuel load and fuel aridity. The value is the median of percent changes within each bin. Panels (e), (f), (g), and (h) show the climate change effect and (i), (j), (k), and (l) show combined climate change and CO_2 fertilization effects (i.e., the overall effect). Region A has low fuel load with a broader range of aridity, representing grasses, region B is dry with low fuel loading, where shrubs dominate, and region C is relatively humid with high fuel loading, where forests dominate. For more information about vegetation distribution of each scenario see Figure S10.

In the 2070s, changes in $\mathbf{P_{burn}}$ were more consistent across storylines and fuel conditions. With climate change, the fuel conditions in Region B (shrub-dominated) and C (evergreen forest) converged with Region A (grass-dominated), where the watershed as a whole became intensely fuel-limited (caused by climate change effect on vegetation growth and litter decomposition). The CO_2 fertilization effect tempered the magnitude of decreasing fuel loads in the 2070s but was not sufficient for changing the direction of $\mathbf{P_{burn}}$, with a few exceptions (e.g., in region A and C under the MultiMean climate change storyline, *Figure 7 i*). However, in Region B, where shrubs were distributed broadly across the whole basin (*Figure 2*), the dominant mechanism differed among climate change storylines.

In all cases, the CO_2 fertilization effect had an upper limit (i.e., around 610 ppm, which was the concentration at the beginning of assessment period for the 2070s) at which it can no longer compete with climate change; as the climate continues to warm and the fuel load continues to decrease, which shifts the system from flammability limited to fuel limited, the mitigating effects of CO_2 fertilization appear to diminish.

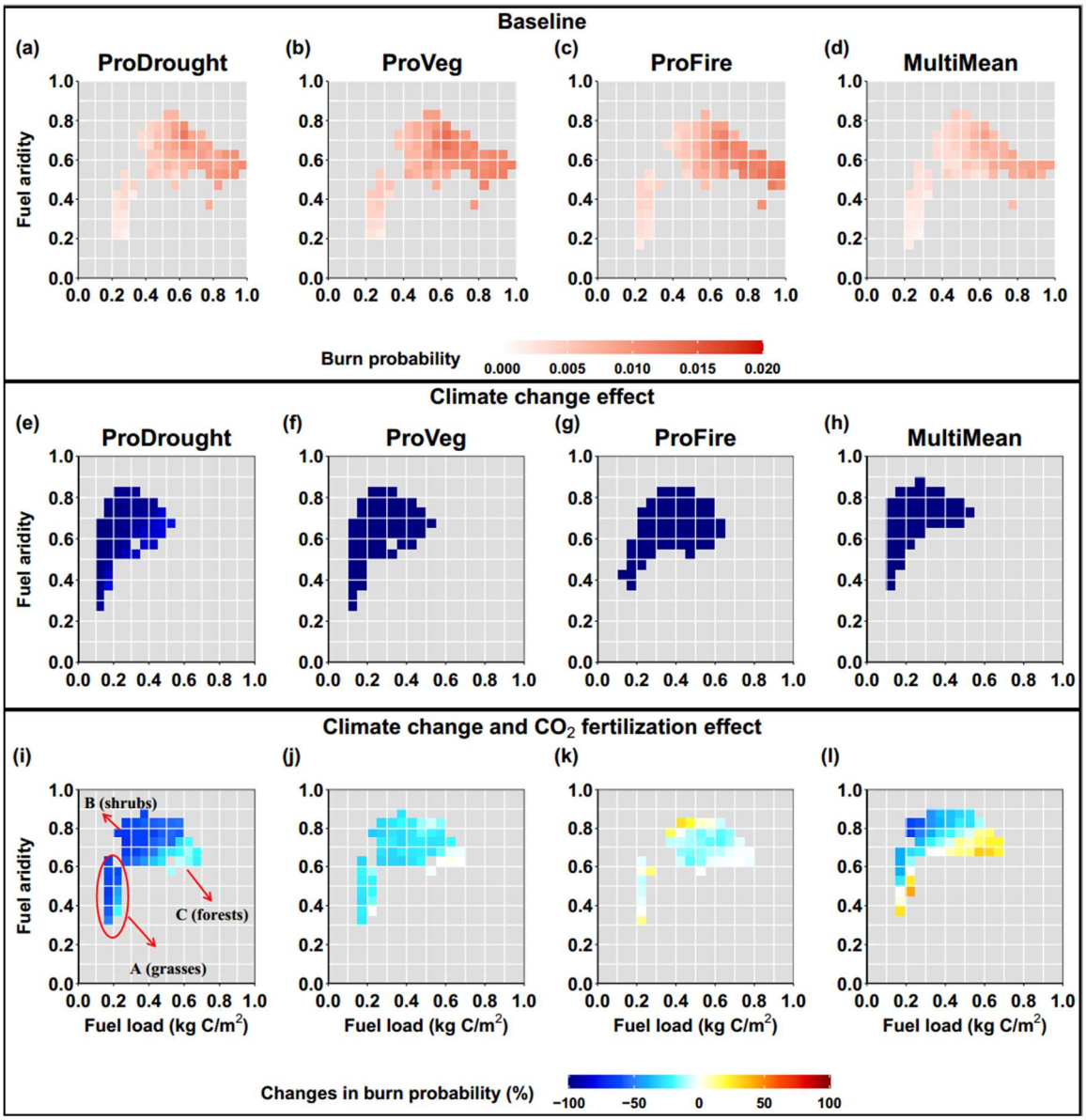

Figure 7. Relationships among fuel load (i.e., litter carbon), fuel aridity, and percentage changes in burn probability (relative to baseline) under various climate change and atmospheric CO_2 fertilization effect scenarios in the 2070s. Panels (a), (b), (c), (d) show the distribution of burn probability against fuel load and fuel aridity for baseline scenario as the reference (the same baseline as 2040s). Other panels show bivariate effects of fuel load and fuel aridity on percentage changes in burn probability (climate change scenario minus baseline scenario). For more information about the vegetation distribution of each bin see Figure S11.

To better understand why the ProDrought and ProVeg storylines exhibit different $\mathbf{P_{burn}}$ responses, we analyzed spatial distributions of $\mathbf{P_{burn}}$, fuel aridity, fuel load, and net primary productivity (NPP) for the baseline and the 2040s scenarios (*Figure 8* and *Figure 9*). Recall that

ProDrought was the only storyline with a mix of increases and decreases in P_{burn} for the overall effect, whereas ProVeg exhibited strong increases across the watershed (*Figure 6*). For the climate change scenario, both GCM storylines decreased fuel loading, but had opposite effects on fuel aridity (i.e., fuel aridity increased under ProDrought, *Figure 8* b; and decreased under ProVeg, *Figure 9* b). Therefore, under ProVeg, decreases in both fuel loading and aridity compounded to decrease $\mathbf{P_{burn}}$ (*Figure 9 a*). Under ProDrought on the other hand, decreases in fuel load and increases in fuel aridity counteracted one another; however, the effects of decreasing fuel loads outstripped increasing fuel aridity to decrease P_{burn} (*Figure 8* a). While both storylines exhibit decreases in P_{burn} across the watershed, this occurred for different reasons. The ProDrought and ProVeg storylines demonstrate the competing and/or compounding effects of exogenous (climate change vs CO_2 fertilization) and endogenous (fuel load vs fuel aridity) drivers.

3.3 Mechanisms driving fire regime changes in the dry future storyline (e.g., ProDrought)

Under the **climate change only scenario and ProDrought** storyline, fuel loading and fuel aridity had counteracting effects on fire regimes and those effects varied among locations. What are the mechanisms that result in fuel load and fuel aridity competing with each other in **the ProDrought** storyline? *Fuel Load:* warming increased NPP and fuel loading in the relatively humid, forested areas and decreased NPP and fuel loading in water-limited areas (*Figure 8* d). However, at the same time, warming decreased fuel loading by increasing decomposition rates in both dry and humid areas (*Figure S5*). Overall decreases in fuel load suggest that decomposition dominates over the increase of NPP in forested area. While some studies corroborate this finding in semiarid systems (Matthews et al., 2012), future decomposition rates are a key source of uncertainty in C cycling models (Luo et al., 2015; Tang & Riley, 2020). Given our current

473 understanding and representation of decomposition under climate change, the net effect,
474 therefore, is a decrease in fuel loading across the basin. *Fuel aridity:* warming increases fuel
475 aridity across the whole basin because it increases PET but not AET since the watershed is
476 largely water-limited (Bradstock, 2010; Littell et al., 2016). *Net Effect:* the decrease in P_{burn}
477 shows that the decrease of fuel load dominates over the increase in fuel aridity.

478 What are the mechanisms that result in climate change and CO_2 fertilization competing
479 with each other in **the ProDrought storyline** for the **Overall Effect**? *Climate Change:* this
480 decreases P_{burn} for the reasons described above. CO_2 fertilization, on the other hand, increased
481 NPP and fuel loading, especially in arid areas (*Figure 8 h*) because the vegetation became more
482 energy- and water- efficient under greater ambient CO_2 concentrations (Becklin et al., 2017). By
483 reviewing evidences from different approaches (field observation and vegetation models), Lewis
484 et al., (2009) also found rising CO_2 concentration is the most likely driver of increased NPP. *Net*
485 *Effect:* fuel loading decreased overall, suggesting that the climate change effect dominates over
486 the CO_2 fertilization effect (*Figure 8* g). CO_2 fertilization also further increased fuel aridity by
487 increasing LAI in water-limited areas (*Figure 8* f). This occurred because greater LAI can
488 intensify the difference between PET and AET for water-limited ecosystems (Tague et al., 2009;
489 Warren et al., 2011). With the overall effect, P_{burn} increased in the relatively humid areas and
490 decreased in the arid area (*Figure 8* i). This suggests that, in the relatively humid areas that are
491 historically flammability-limited, increases in fuel aridity can increase fire activity even with
492 reduced fuel loading. However, in arid areas, fire activity is more sensitive to changes in fuel
493 load than fuel aridity (*Figure 8* i).

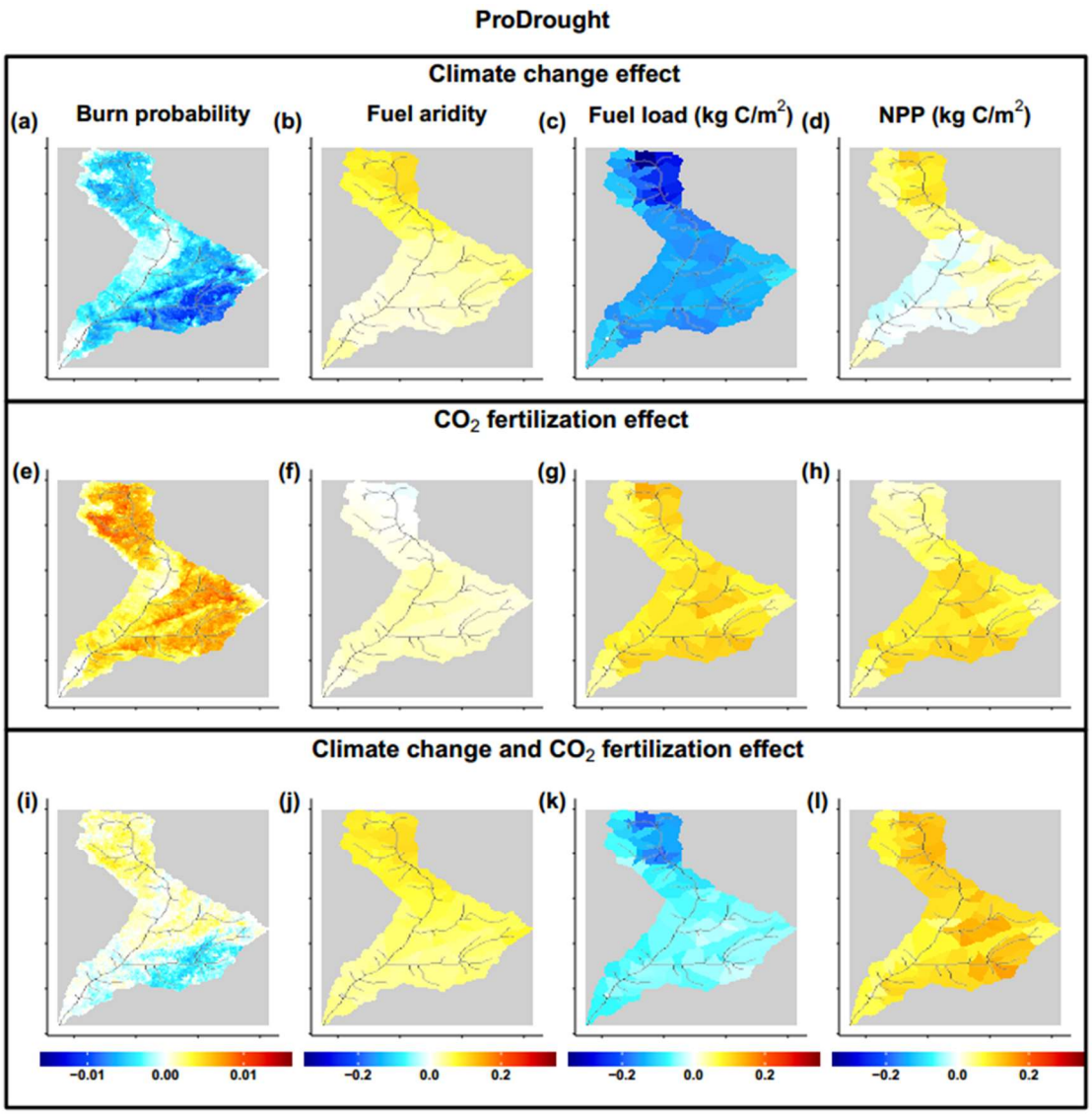

494

495 *Figure 8. The individual and combination effect of climate change and CO_2 fertilization on burn*
496 *probability, mean annual fuel aridity, mean annual fuel load (i.e., litter carbon), and mean*
497 *annual NPP over the 30 years' assessment period in the 2040s under the ProDrought climate*
498 *change storyline (effects are calculated as the difference between future scenario and baseline).*
499 *Red colors represent increases; blue colors represent decreases. Panels (a), (e), and (i) are*
500 *changes in burn probability; panels (b), (f), and (j) are changes in fuel aridity; panels (c), (j),*
501 *and (k) are changes in fuel load; and panels (d), (h), and (i) are changes in NPP.*
502

503 3.4 Mechanisms driving fire regime changes in the wet future storylines (e.g., ProVeg)

504 What are the mechanisms that result in climate change and CO_2 fertilization competing

505 with each other **in the ProVeg storyline for the Overall Effect**? *Climate Change:* both fuel

loading and fuel aridity decreased (*Figure 9 b* & *c*). Fuel loading decreased in response to warming while more precipitation decreased aridity (*Figure S12*). *CO_2 Fertilization:* as with all storylines, CO_2 fertilization increased fuel loading. However, it had a mixed effect on fuel aridity, with slight increases occurring in more the arid areas and slight decreases occurring in the more humid areas (*Figure 9 f*). *Net Effect*: We observed a net increase in fuel loading, suggesting that CO_2 fertilization can dominate over climate change-induced drought under wetter future scenarios (*Figure 9 k*). For fuel aridity, CO_2 fertilization only outstripped the climate change effect in very arid areas (at the bottom part of the basin, CO_2 fertilization changed the fuel aridity from a decrease to an increase, *Figure 9 j*). P_{burn} increased across the entire basin (even with less arid fuel), indicating that increasing fuel load was the main driver of P_{burn} for the **overall effect, under the ProVeg storyline** (*Figure 9 i*).

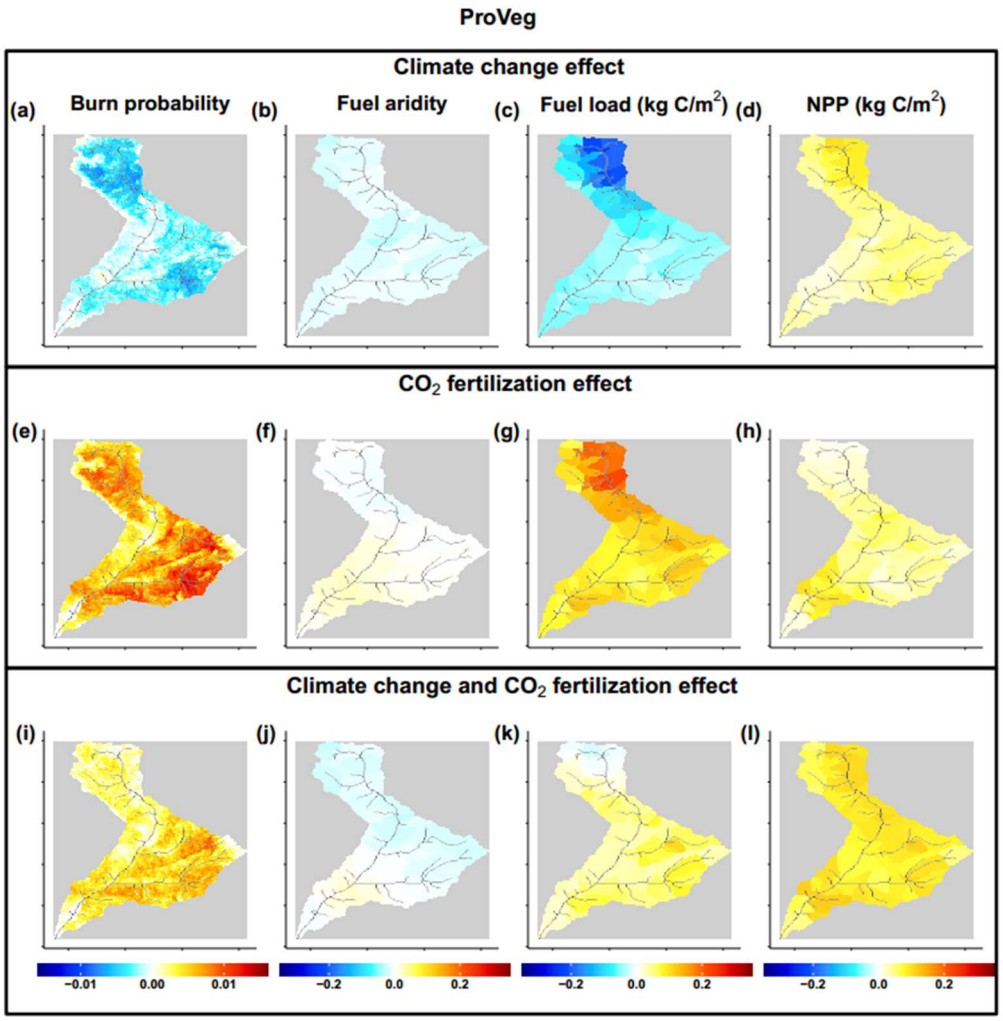

Figure 9. The individual and combined effects of climate change and CO_2 fertilization on burn probability, mean annual fuel aridity, mean annual fuel load (i.e., litter carbon), and mean annual NPP over 30 years' assessment period in the 2040s under the ProVeg climate change storyline. The red colors indicate increases; blue colors indicate decreases. Panel (a), (e), and (i) are changes in burn probability; panels (b), (f), and (j) are changes in fuel aridity; panels (c), (j), and (k) are changes in fuel load; and panels (d), (h), and (i) are changes in NPP.

4 Discussion

Vegetation productivity and litter decomposition are critical processes that integrate exogenous and endogenous drivers (e.g., climate and fuels) to shape wildfire activity. For example, we found that in the mid-21st century (2040s), CO_2 fertilization increased NPP to a greater extent than it was reduced by climate change-induced drought, resulting in a net increase

in fuel loading and resultant fire activity. However, by the late-21st century (2070s), climatic warming (and associated drought) outstripped the effects of CO_2 fertilization, leading to a decrease in fire activity. The timing and magnitude of these trade-offs were modified by local aridity gradients and vegetation composition. This local-scale variability, combined with the non-monotonic responses we observed, suggest that we cannot linearly or empirically extrapolate fire activity from the baseline and 2040s scenarios to the 2070s (Balshi et al., 2009; Westerling et al., 2011). Projecting future fire regimes requires accounting for complex feedbacks among climate, hydrology, vegetation productivity and biogeochemical processes.

Climate change and increasing CO_2 are the main drivers of future fire regimes, through their direct impact on biophysical processes and indirect effects on vegetation dynamics and biogeochemical processes. Below, we summarize the main drivers of fire regimes, how they interact to influence future fire regimes, and how these interactions vary with precipitation patterns and local aridity gradients (*Figure 10*).

4.1 The role of exogenous drivers in influencing future fire regimes

4.1.1 The role of climate change and CO_2 fertilization in influencing future fire regimes

Exogenous drivers affect fire regimes through their effects on vegetation productivity, litter decomposition, and endogenous fire drivers (i.e., fuel loading and fuel aridity; Kennedy et al., 2021). Climate warming and CO_2 fertilization are two key exogenous drivers that can either compete with or compound one another to influence fire regimes. For example, given sufficient moisture, climate warming can increase vegetation growth and fuel loading by increasing photosynthetic activity (Kurz et al., 2008). However, warming can also accelerate litter decomposition, which can counteract such increases (Bradstock, 2010; Keane et al., 1999; Kurz

et al., 2008). We found that in Trail Creek, this model system predicts that litter decomposition dominated over increases in vegetation productivity (*Figure 8* c and *Figure 9* c).

Aridity and CO_2 fertilization can also compete to influence fuel and fire dynamics. In water-limited locations for example, climate change can actually decrease fuel loading and fire activity by promoting drought (Hanan et al. 2021). CO_2 fertilization can enhance vegetation productivity and resultant fire activity by enabling higher rates of photosynthesis when stomata are partially closed to reduce transpiration (Becklin et al., 2017; Lewis et al., 2009). Consequently, drought effects on plant productivity can be tempered by CO_2 fertilization, and the final fuel loading is determined by two competing mechanisms: climate change and CO_2 fertilization. We found that the ProVeg and ProDrought storylines led to different fuel loadings, which suggests precipitation patterns (and aridity) play a strong role in the relative balance between these mechanisms (*Figure 8 k* and *Figure 9 k*).

Climate warming and CO_2 fertilization can also compound one another to influence fuel aridity. For example, in water-limited ecosystems, climate warming can increase the water budget deficit (i.e., PET – ET, Bradstock, 2010; Littell et al., 2016), while CO_2 fertilization can increase leaf area index and PET thus making plants more water stressed (Warren, et al. 2011; Tague, et al. 2009). However, this compounding effect is location-dependent and can be modified by precipitation patterns, which will be discussed in the next section (*Figure 8 j* and *Figure 9 j*).

Our modeling results suggest that plant responses to CO_2 fertilization are an important factor in predicting future fire regimes in fuel-limited watersheds such as Trail Creek. Physiological responses to rising CO_2 can vary among species and over time and there is still a great deal of uncertainty in projecting physiological responses to increasing atmospheric CO_2

because empirical studies have produced mixed results (Becklin et al., 2017; Lewis et al., 2009; Norby et al., 2016; Warren et al., 2011). RHESSys accounts for the direct effect of increasing water use efficiency on assimilation and the resulting potential increases in growth and biomass (including LAI). However, other responses such as changes in stomatal functioning under elevated CO_2 (Swann et al., 2016) or changes in allocation or leaf physiology (Warren et al., 2011) were not included, and may dampen or alter projected CO_2 fertilization changes. Our no-CO_2 vs. CO_2 fertilization scenarios account for the two extreme possibilities, when reality may be somewhere in the middle.

Litter stores are a major control on fire spread. Thus, modeling fire spread requires high skill in representing litterfall and decomposition. Decomposition in particular is complex and is affected by temperature, moisture, nitrogen, pH, and microbial dynamics (Lin & Webster, 2014). Although RHESSys accounts for many of these drivers, it necessarily includes some simplifications that may ignore important mechanisms in semiarid, fire-prone systems. For example, spatial partitioning of moisture and nitrogen in litter stores can accelerate or decelerate decomposition during drying and rewetting cycles (Birch, 1959). Hanan et al., (2021, submitted) also found that the sensitivity of modeled decomposition rate to parameter and model structure uncertainties increases with climate warming but decreases with increasing precipitation. This may be problematic when projecting the future fuel load under climate change. Especially, these uncertainties can compound each other when the projection period is longer, thus causing more uncertainties when extends the projections from 2040s to 2070s.

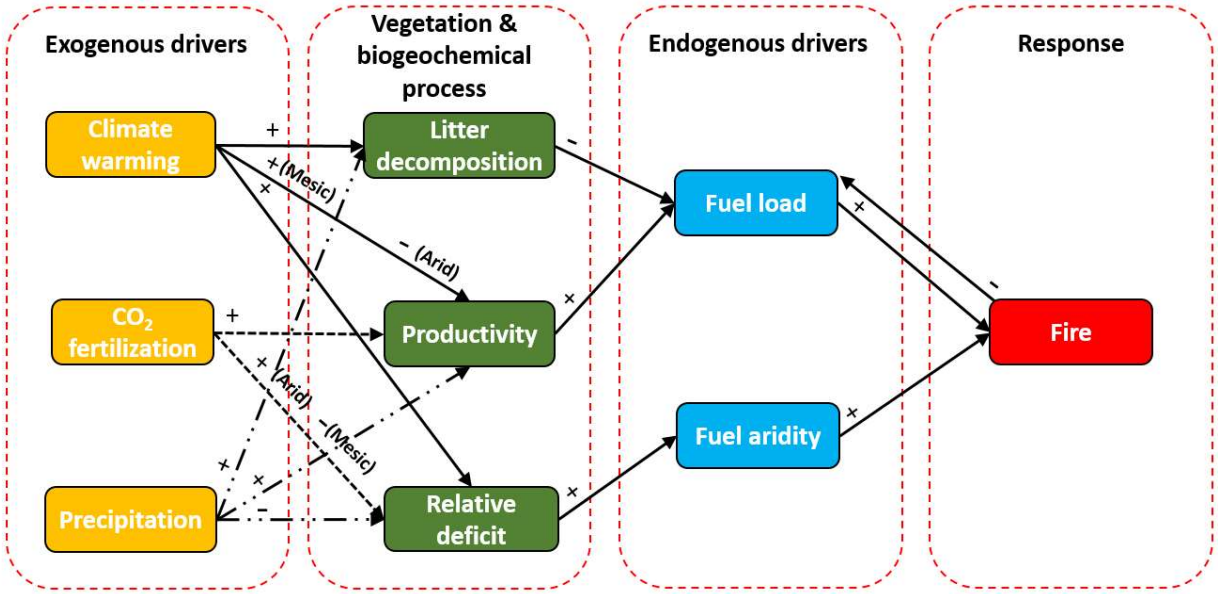

Figure 10. Conceptual diagram illustrating how exogenous drivers, vegetation, litter decomposition and endogenous drivers interact to influence wildfire burn probability. "+" indicates an increase (e.g., increases in productivity cause increases in fuel loading; "-" indicates a decrease (e.g., increases in litter decomposition lead to decreases in fuel loading). "Mesic" and "arid" indicates that the specified affect is location dependent and occurs in mesic or arid locations. Relative deficit is calculated as (1 – ET)/PET.

4.1.2 The role of precipitation in influencing future fire regimes

Precipitation was also an important factor in predicting future fire regimes in our relatively fuel-limited watershed. At an annual timescale, increases in precipitation can decrease fire activity by increasing fuel moisture and decreasing the length of the fire season. However, over longer timescales, increased precipitation can increase fuel loading and resultant fire activity. Other studies have also found that precipitation is important in driving fuel load and fire (Bradstock, 2010; Littell et al., 2016; Pausas & Paula, 2012; Williams et al., 2019). Recent research has also shown that, in a drier future, there may be less fire due to decreases in fuel loading; whereas in a wetter future, there may be more fire activity due to increases in productivity, *Figure 10)*. Williams et al., (2019) also argue that interannual variability (i.e., the sequencing of dry and wet extremes) is as important as changes in average precipitation. A

613 worst-case scenario for a fuel-limited system would be a high precipitation year followed by a
614 low precipitation year, in which the wet year increases fuel abundance and the dry year provides
615 the arid conditions needed to cause large fires (Kennedy, 2019; Williams et al., 2019). This is the
616 sequence that currently drives large fire growth in the arid southwestern US, and will likely
617 expand in extent under climate change (Abatzoglou & Kolden, 2011).

618 Despite its importance, particularly in semi-arid systems, there is considerable
619 uncertainty in prediction of future precipitation patterns among GCMs (Pendergrass et al., 2017;
620 Polade et al., 2017). Our study shows that ProVeg increases fire activity in 2040s to the greatest
621 extent compared to other GCMs. During fire season, ProVeg had a 6% increase in precipitation,
622 while other storylines had decreases (*Figure S12*). We found that higher precipitation increased
623 productivity and fuel loads, thereby increasing fire activity (*Figure 10;* Kennedy et al., 2021),
624 and that, for Trail Creek, precipitation is as critical in driving future fire regimes as warming
625 (e.g., *Figure 8 d* vs. *Figure 9 d*).

626 4.2 The role of endogenous drivers in influencing future fire regimes

627 Fuel loading and fuel aridity can also counteract one another driving future fire regimes,
628 and their interactions are also modified by vegetation type. For example, we found that increases
629 in fuel aridity could increase fire activity but these increases were tempered by decreases in fuel
630 loading. This is consistent with conceptual frameworks that describe gradual transitions from
631 forests and shrub lands to grasslands due to fire-climate feedbacks (e.g., Bowman et al., 2020).
632 Plant functional types (grass, shrub and forest) are generally distributed along gradients in aridity
633 and productivity leading to differences in their fire regimes, and the sensitivity of fire regimes to
634 climate change (Bradstock, 2010; Littell et al., 2016; Williams et al., 2019). For example,
635 woodland fires in dry climates are limited by fuel loads, and forest fires in wet climates are

limited by fuel moisture (Bradstock, 2010). To explore the role of vegetation type in affecting fuel conditions for driving future fire activity, we calculate changes in P_{burn} in response to changes in fuel loading (Δ*fuel loading)* and changes in fuel aridity (Δ*fuel aridity*) for each vegetation type (*Figure 11*). For all vegetation types, when fuel load and aridity both increased, they compounded to increase P_{burn}. However, as fuel load decreased, and fuel aridity increased, the dominant driver varied among vegetation type. We investigated this difference by drawing a line in each panel that separated negative and positive changes in P_{burn}. For conifer and shrub patches, the line had a negative slope (Δ*fuel loading:*Δ *fuel aridity* is 1:1), which represents a threshold separating the negative and positive changes in P_{burn}. A sloped line indicates that both fuel load and fuel aridity drive P_{burn} therefore conifer stands in Trail Creek (region C in *Figure 6*) can be classified as co-limited by fuel and flammability. While many previous studies using empirical models suggest that forest fire activity will increase under future warming due to increases in fuel aridity (Bradstock 2010), our process-based model results agrees with conceptual frameworks and suggest that in semiarid forests, fire activity may ultimately decrease due to decreasing fuel loads (even without wildfire-driven self-limitation) despite increases in fuel aridity. These results are corroborated by studies in other dry forests that similarly found fire activity is likely to decrease in the future due to drought (Halofsky et al., 2020; Littell et al., 2018). In *grass-dominated locations,* the line that separates P_{burn} increases or decreases is vertical, which indicates that this area is fuel-limited and fuel load is the main driver of P_{burn} (i.e. P_{burn} is insensitive to changes in fuel aridity, vertical line in *Figure 11 c* and *f*). Each vegetation type shows its own pattern of fire responses to climate change; fire in dry woodland ecosystem is limited by fuel loading, while fire in wet forest is limited by fuel aridity and fire weather (Bradstock, 2010).

659 The lines separating the negative and positive changes in P_{burn} have the same pattern in
660 the 2070s as for the 2040s, indicating that they represent a consistent characteristic of this
661 watershed over time (assuming no vegetation type-conversion). In the 2070s, we see the cluster
662 of patches moves towards lower fuel loading (to the left), and higher fuel aridity (upwards).
663 Therefore, even though we observed a non-monotonic trend in fire response to climate change
664 from the 2040s to 2070s (*Figure 4* and *Figure 5*), here we found that the Δ*fuel loading:*Δ *fuel*
665 *aridity threshold,* above which increases in fuel aridity dominate over decreases in fuel loading
666 (and vice versa), is stationary, and this stationary threshold varies among vegetation types (pines
667 and shrubs show a similar pattern while grasses stand out as highly fuel-limited). In evergreen
668 forest ecosystems, for patches above the threshold line, P_{burn} increases with higher fuel aridity
669 meaning that increases in fuel aridity dominated over the decreases in fuel loading (*Figure 11 a*).
670 In grass ecosystems, fuel loading was the only factor that separated increases or decreases in
671 P_{burn} (*Figure 11 c*). Because the distribution of plant functional types is shifting in many
672 locations due to climate change (Batllori et al., 2020), identifying the stationary threshold for
673 new vegetation types may be useful for predicting future fire regimes.

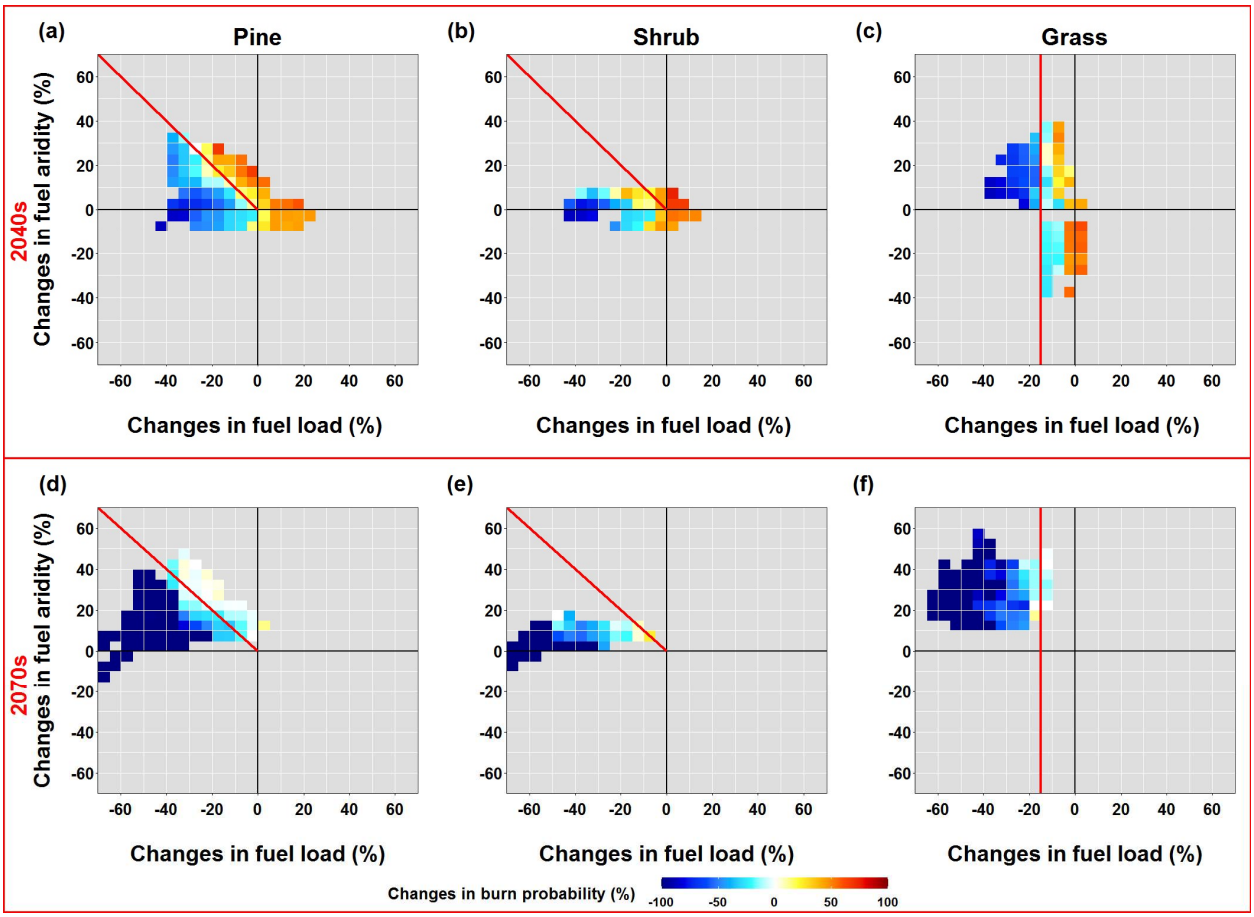

Figure 11. The changes in burn probability in response to changes of fuel load and fuel aridity (in percentage) relative to the baseline. (a), (b), and (c) illustrate how burn probability changes in response to changes in fuel load and fuel aridity for 2040s. (d), (e), and (f) show responses for 2070s. Changes are binned by every 5 percent change, and changes in burn probability are the median of these bins (note that the data for these bins are drawn from all four GCM storylines). We removed bins that had less than 100 observations. The panels are as follows: a&d: pine; b&e: shrub; and c&f: grass. All these changes are between future climate change and CO_2 fertilization scenarios and the baseline scenario. The red line is the threshold Δfuel loading:Δ fuel aridity that separates negative and positive changes in burn probability.

4.3 The role of aridity gradient in influencing future fire regimes

Interactions between exogenous and endogenous drivers can vary along aridity gradients (*Figure 10*). Although top-down climate warming can be the dominant driver of wildfire at large scales, local aridity (P/PET, *Figure 2*) also responds to bottom-up drivers such as topography and vegetation composition (Hanan et al., 2021; Littell et al., 2018). As a result, climate warming can

690 have different effects on fuel loading in arid vs. mesic locations (e.g., *Figure 8 d*). In arid
691 locations, warming can increase drought stress and reduce productivity and resultant fuel
692 loading, while in more mesic locations warming can increase productivity by increase
693 photosynthetic activity. Similarly, the effects of CO_2 fertilization also differ between arid and
694 mesic locations (e.g., *Figure 9 f*). In water-limited locations, CO_2 fertilization can increase fuel
695 aridity by increasing leaf area index and therefore water deficit (as explained in previous section
696 4.1). In mesic locations, CO_2 fertilization is more likely to decrease fuel aridity by increasing ET,
697 thereby decreasing water deficit (Warren et al. 2011; Duursma et al. 2014; Becklin et al. 2017).
698 To further complicate matters, aridity gradients are not stationary under climate change. With
699 warming, some historically mesic areas are likely to become increasingly arid (Abatzoglou &
700 Kolden, 2011; Goss et al., 2020; McKenzie & Littell, 2017). Thus, interactions between
701 exogenous and endogenous drivers can vary over space and time. It is worth noting, however,
702 that as the frequency and mean size of very large fires increases, single fires regularly burn
703 across these gradients, further challenging the ability to model fire-climate-vegetation feedbacks
704 that are already difficult to disentangle.

705 **5 Conclusions**

706 We found that climate change and CO_2 fertilization effects can counteract one another to
707 alter fuel loads. Climatic warming reduced fuel loading by decreasing vegetation productivity
708 and increasing fuel decomposition rates, while CO_2 fertilization increased fuel loading by
709 enhancing vegetation productivity. On the other hand, both climatic warming and CO_2
710 fertilization increased fuel aridity. In the 2040s, CO_2 fertilization outstripped climatic warming to
711 increase fire activity; however, in the 2070s, climatic warming became so intense that the
712 mitigating effects of CO_2 fertilization could no longer keep up and therefore, fire activity

713 decreased. This non-monotonic response in fire size and burn probability occurred because
714 decreases in fuel loading dominated over the increases in fuel aridity. However, the decreases in
715 fuel loading will outstrip changes in fire weather and causes a 100% reduction in wildfire under
716 the climate change in the far future (2070s) seems like a radical result. Some important feedback
717 or threshold may be missing when modeling the effect of climate change on decomposition. But
718 our simulation study does provide interesting possibilities in how climate and vegetation interact
719 with wildfire, particularly in the context of increasing atmospheric CO_2 concentration.

720 Vegetation type is an important factor modifying how future fire regimes respond to
721 tradeoffs between fuel loading and aridity. For example, Δ*fuel loading:*Δ *fuel aridity* thresholds
722 that determine whether fire regimes are influenced more by fuel loading or fuel aridity vary
723 between grasses (in which fuel load is limiting) and conifer and shrub stands (where fuel load
724 and fuel aridity can both be limiting depending on underlying aridity gradients). For all
725 vegetation types, this threshold does not change between the 2040s and the 2070s, suggesting
726 that thresholds are a stationary characteristic of a given vegetation type. This stationary threshold
727 can be used as a tool to predict future fire regimes.

728 Given the catastrophic consequences of wildfire to human infrastructure, identifying
729 appropriate management actions to reduce vulnerability is a high priority. However, fire regimes
730 are changing (Littell et al., 2018; Liu et al., 2013; Liu & Wimberly, 2016), and therefore,
731 allocation of limited resources to reduce fire risks and societal vulnerability will need to take
732 these changes into account. Our modeling approach demonstrates that fire regimes will likely
733 change differentially across watersheds, but there is still substantial uncertainty in the models. As
734 scientists work to reduce key uncertainties—including future precipitation patterns, future

decomposition rates, and species-specific responses to CO_2 fertilization—future projections will continue to be refined, providing better support to wildfire management decisions.

Acknowledgments

This project is supported by National Science Foundation of United States under award numbers DMS-1520873 and DEB-1916658. William Burke and Tung Nguyen provided helpful support for setting up the RHESSys model. We thank Jan Boll, Nicholas Engdahl, Rebecca Gustine, and Ames Fowler for providing valuable suggestions on the manuscript.

Code and data availability

The coupled RHESSys-WMFire model code is available online at: https://doi.org/10.5281/zenodo.5594757 (Ren et al., 2021a). The data used in this study are available at: https://doi.org/10.17605/OSF.IO/AX45N (Ren et al., 2021b).

References

Abatzoglou, J. T., Kolden, C. A., DiMento, J. F. C., Doughman, P., & Nespor, S. (2014). Cliamte-change effects, adaptation, and mitigation. In *Climate Change: what IT Means for Us, Our Children, and Our Grandchildren.* (pp. 53–104). MIT Press.

Abatzoglou, John T. (2013). Development of gridded surface meteorological data for ecological applications and modelling. *International Journal of Climatology*, *33*(1), 121–131. https://doi.org/10.1002/joc.3413

Abatzoglou, John T., & Brown, T. J. (2012). A comparison of statistical downscaling methods suited for wildfire applications. *International Journal of Climatology*, *32*(5), 772–780. https://doi.org/10.1002/joc.2312

Abatzoglou, John T., & Kolden, C. A. (2011). Climate Change in Western US Deserts: Potential for Increased Wildfire and Invasive Annual Grasses. *Rangeland Ecology & Management*, *64*(5), 471–478. https://doi.org/10.2111/REM-D-09-00151.1

Abatzoglou, John T., & Kolden, C. A. (2013). Relationships between climate and macroscale area burned in the western United States. *International Journal of Wildland Fire*, *22*(7), 1003. https://doi.org/10.1071/WF13019

Abatzoglou, John T., & Rupp, D. E. (2017). Evaluating climate model simulations of drought for the northwestern United States. *International Journal of Climatology*, n/a-n/a. https://doi.org/10.1002/joc.5046

Abatzoglou, John T., & Williams, A. P. (2016). Impact of anthropogenic climate change on wildfire across western US forests. *Proceedings of the National Academy of Sciences*, *113*(42), 11770–11775. https://doi.org/10.1073/pnas.1607171113

768 Abatzoglou, John T., Williams, A. P., & Barbero, R. (2019). Global Emergence of
769 Anthropogenic Climate Change in Fire Weather Indices. *Geophysical Research Letters*,
770 *46*(1), 326–336. https://doi.org/10.1029/2018GL080959
771 Balshi, M. S., Mcguire, A. D., Duffy, P., Flannigan, M., Kicklighter, D. W., & Melillo, J. (2009).
772 Vulnerability of carbon storage in North American boreal forests to wildfires during the
773 21st century. *Global Change Biology*, *15*(6), 1491–1510. https://doi.org/10.1111/j.1365-
774 2486.2009.01877.x
775 Bart, R. R., Kennedy, M. C., Tague, C. L., & McKenzie, D. (2020). Integrating fire effects on
776 vegetation carbon cycling within an ecohydrologic model. *Ecological Modelling*, *416*,
777 108880. https://doi.org/10.1016/j.ecolmodel.2019.108880
778 Batllori, E., Lloret, F., Aakala, T., Anderegg, W. R. L., Aynekulu, E., Bendixsen, D. P., et al.
779 (2020). Forest and woodland replacement patterns following drought-related mortality.
780 *Proceedings of the National Academy of Sciences*.
781 https://doi.org/10.1073/pnas.2002314117
782 Becklin, K. M., Walker, S. M., Way, D. A., & Ward, J. K. (2017). CO2 studies remain key to
783 understanding a future world. *New Phytologist*, *214*(1), 34–40.
784 https://doi.org/10.1111/nph.14336
785 Birch, H. F. (1959). Further observations on humus decomposition and nitrification. *Plant and*
786 *Soil*, *11*(3), 262–286. https://doi.org/10.1007/BF01435157
787 Bowman, D., Kolden, C., Abatzoglou, J., Johnston, F., Werf, G., & Flannigan, M. (2020).
788 Vegetation fires in the Anthropocene. *Nature Reviews Earth & Environment*, *1*, 1–16.
789 https://doi.org/10.1038/s43017-020-0085-3

Bradstock, R. A. (2010). A biogeographic model of fire regimes in Australia: current and future implications. *Global Ecology and Biogeography*, *19*(2), 145–158. https://doi.org/10.1111/j.1466-8238.2009.00512.x

Buhidar, B. B. (2001). The Big Wood River Watershed Management Plan. *Idaho Department of Environmental Quality, Twin Falls Regional Office, Twin Falls, ID*.

Chaney, N. W., Wood, E. F., McBratney, A. B., Hempel, J. W., Nauman, T. W., Brungard, C. W., & Odgers, N. P. (2016). POLARIS: A 30-meter probabilistic soil series map of the contiguous United States. *Geoderma*, *274*, 54–67. https://doi.org/10.1016/j.geoderma.2016.03.025

Cohen, J. D., & Deeming, J. (2006). *National Fire Danger Rating System (NFDRS)*. American Cancer Society. https://doi.org/10.1002/0471743984.vse8649

Daly, C., Neilson, R. P., & Phillips, D. L. (1994). A Statistical-Topographic Model for Mapping Climatological Precipitation over Mountainous Terrain. *Journal of Applied Meteorology*, *33*(2), 140–158. https://doi.org/10.1175/1520-0450(1994)033<0140:ASTMFM>2.0.CO;2

Dewitz, J. (2019). National Land Cover Database (NLCD) 2016 Products. U.S. Geological Survey data release. Retrieved from https://doi.org/10.5066/P96HHBIE

Duursma, R. A., Barton, C. V. M., Lin, Y.-S., Medlyn, B. E., Eamus, D., Tissue, D. T., et al. (2014). The peaked response of transpiration rate to vapour pressure deficit in field conditions can be explained by the temperature optimum of photosynthesis. *Agricultural and Forest Meteorology*, *189–190*, 2–10. https://doi.org/10.1016/j.agrformet.2013.12.007

Farquhar, G. D., & von Caemmerer, S. (1982). Modelling of Photosynthetic Response to Environmental Conditions. In O. L. Lange, P. S. Nobel, C. B. Osmond, & H. Ziegler

812 (Eds.), *Physiological Plant Ecology II: Water Relations and Carbon Assimilation* (pp.
813 549–587). Berlin, Heidelberg: Springer. https://doi.org/10.1007/978-3-642-68150-9_17
814 Flitcroft, R. L., Falke, J. A., Reeves, G. H., Hessburg, P. F., McNyset, K. M., & Benda, L. E.
815 (2016). Wildfire may increase habitat quality for spring Chinook salmon in the
816 Wenatchee River subbasin, WA, USA. *Forest Ecology and Management*, *359*, 126–140.
817 https://doi.org/10.1016/j.foreco.2015.09.049
818 Frenzel, S. A. (1989). *Water resources of the upper Big Wood River basin, Idaho*. US Geological
819 Survey.
820 Garcia, E. S., & Tague, C. L. (2015). Subsurface storage capacity influences climate–
821 evapotranspiration interactions in three western United States catchments. *Hydrology and*
822 *Earth System Sciences*, *19*(12), 4845–4858. https://doi.org/10.5194/hess-19-4845-2015
823 Goss, M., Swain, D. L., Abatzoglou, J. T., Sarhadi, A., Kolden, C., Williams, A. P., &
824 Diffenbaugh, N. S. (2020). Climate change is increasing the risk of extreme autumn
825 wildfire conditions across California. *Environmental Research Letters*.
826 https://doi.org/10.1088/1748-9326/ab83a7
827 Halofsky, J. E., Peterson, D. L., & Harvey, B. J. (2020). Changing wildfire, changing forests: the
828 effects of climate change on fire regimes and vegetation in the Pacific Northwest, USA.
829 *Fire Ecology*, *16*(1), 4. https://doi.org/10.1186/s42408-019-0062-8
830 Hanan, E. J., Tague, C. (Naomi), & Schimel, J. P. (2017). Nitrogen cycling and export in
831 California chaparral: the role of climate in shaping ecosystem responses to fire.
832 *Ecological Monographs*, *87*(1), 76–90. https://doi.org/10.1002/ecm.1234
833 Hanan, E. J., Tague, C., Choate, J., Liu, M., Kolden, C., & Adam, J. (2018). Accounting for
834 disturbance history in models: using remote sensing to constrain carbon and nitrogen pool

spin-up. *Ecological Applications: A Publication of the Ecological Society of America*, *28*(5), 1197–1214. https://doi.org/10.1002/eap.1718

Hanan, E. J., Ren, J., Tague, C. L., Kolden, C. A., Abatzoglou, J. T., Bart, R. R., et al. (2021). How climate change and fire exclusion drive wildfire regimes at actionable scales. *Environmental Research Letters*, *16*(2), 024051. https://doi.org/10.1088/1748-9326/abd78e

Hicke, J. A., Johnson, M. C., Hayes, J. L., & Preisler, H. K. (2012). Effects of bark beetle-caused tree mortality on wildfire. *Forest Ecology and Management*, *271*, 81–90. https://doi.org/10.1016/j.foreco.2012.02.005

Jarvis, P. G. (1976). The Interpretation of the Variations in Leaf Water Potential and Stomatal Conductance Found in Canopies in the Field. *Philosophical Transactions of the Royal Society B: Biological Sciences*, *273*(927), 593–610. https://doi.org/10.1098/rstb.1976.0035

Keane, R. E., Morgan, P., & White, J. D. (1999). Temporal patterns of ecosystem processes on simulated landscapes in Glacier National Park, Montana, USA. *Landscape Ecology*, *14*(3), 311–329. https://doi.org/10.1023/A:1008011916649

Kennedy, M. C. (2019). Experimental design principles to choose the number of Monte Carlo replicates for stochastic ecological models. *Ecological Modelling*, *394*, 11–17. https://doi.org/10.1016/j.ecolmodel.2018.12.022

Kennedy, M. C., McKenzie, D., Tague, C., & Dugger, A. L. (2017). Balancing uncertainty and complexity to incorporate fire spread in an eco-hydrological model. *International Journal of Wildland Fire*, *26*(8), 706–718. https://doi.org/10.1071/WF16169

857 Kennedy, M. C., Bart, R. R., Tague, C. L., & Choate, J. S. (2021). Does hot and dry equal more
858 wildfire? Contrasting short- and long-term climate effects on fire in the Sierra Nevada,
859 CA. *Ecosphere*, *12*(7), e03657. https://doi.org/10.1002/ecs2.3657
860 Kurz, W. A., Stinson, G., & Rampley, G. (2008). Could increased boreal forest ecosystem
861 productivity offset carbon losses from increased disturbances? *Philosophical*
862 *Transactions of the Royal Society B: Biological Sciences*, *363*(1501), 2259–2268.
863 https://doi.org/10.1098/rstb.2007.2198
864 Lewis, S. L., Lloyd, J., Sitch, S., Mitchard, E. T. A., & Laurance, W. F. (2009). Changing
865 Ecology of Tropical Forests: Evidence and Drivers. *Annual Review of Ecology,*
866 *Evolution, and Systematics*, *40*(1), 529–549.
867 https://doi.org/10.1146/annurev.ecolsys.39.110707.173345
868 Lin, L., & Webster, J. R. (2014). Detritus decomposition and nutrient dynamics in a forested
869 headwater stream. *Ecological Modelling*, *293*, 58–68.
870 https://doi.org/10.1016/j.ecolmodel.2013.12.013
871 Lin, L., Band, L. E., Vose, J. M., Hwang, T., Miniat, C. F., & Bolstad, P. V. (2019). Ecosystem
872 processes at the watershed scale: Influence of flowpath patterns of canopy ecophysiology
873 on emergent catchment water and carbon cycling. *Ecohydrology*, *0*(0), e2093.
874 https://doi.org/10.1002/eco.2093
875 Littell, J. S., Peterson, D. L., Riley, K. L., Liu, Y., & Luce, C. H. (2016). A review of the
876 relationships between drought and forest fire in the United States. *Global Change*
877 *Biology*, *22*(7), 2353–2369. https://doi.org/10.1111/gcb.13275

878 Littell, J. S., McKenzie, D., Wan, H. Y., & Cushman, S. A. (2018). Climate Change and Future
879 Wildfire in the Western United States: An Ecological Approach to Nonstationarity.
880 *Earth's Future*, *6*(8), 1097–1111. https://doi.org/10.1029/2018EF000878
881 Liu, Y., L. Goodrick, S., & A. Stanturf, J. (2013). Future U.S. wildfire potential trends projected
882 using a dynamically downscaled climate change scenario. *Forest Ecology and*
883 *Management*, *294*, 120–135. https://doi.org/10.1016/j.foreco.2012.06.049
884 Liu, Z., & Wimberly, M. C. (2016). Direct and indirect effects of climate change on projected
885 future fire regimes in the western United States. *Science of The Total Environment*, *542*,
886 65–75. https://doi.org/10.1016/j.scitotenv.2015.10.093
887 McCarley, T. R., Kolden, C. A., Vaillant, N. M., Hudak, A. T., Smith, A. M. S., & Kreitler, J.
888 (2017). Landscape-scale quantification of fire-induced change in canopy cover following
889 mountain pine beetle outbreak and timber harvest. *Forest Ecology and Management*, *391*,
890 164–175. https://doi.org/10.1016/j.foreco.2017.02.015
891 McKenzie, D., & Littell, J. S. (2017). Climate change and the eco-hydrology of fire: Will area
892 burned increase in a warming western USA? *Ecological Applications*, *27*(1), 26–36.
893 https://doi.org/10.1002/eap.1420
894 McKENZIE, D., Gedalof, Z., Peterson, D. L., & Mote, P. (2004). Climatic Change, Wildfire, and
895 Conservation. *Conservation Biology*, *18*(4), 890–902. https://doi.org/10.1111/j.1523-
896 1739.2004.00492.x
897 McVicar, T. R., Roderick, M. L., Donohue, R. J., Li, L. T., Van Niel, T. G., Thomas, A., et al.
898 (2012). Global review and synthesis of trends in observed terrestrial near-surface wind
899 speeds: Implications for evaporation. *Journal of Hydrology*, *416–417*, 182–205.
900 https://doi.org/10.1016/j.jhydrol.2011.10.024

Meinshausen, M., Smith, S. J., Calvin, K., Daniel, J. S., Kainuma, M. L. T., Lamarque, J.-F., et al. (2011). The RCP greenhouse gas concentrations and their extensions from 1765 to 2300. *Climatic Change*, *109*(1), 213. https://doi.org/10.1007/s10584-011-0156-z

Mu, Q., Zhao, M., & Running, S. W. (2011). Improvements to a MODIS global terrestrial evapotranspiration algorithm. *Remote Sensing of Environment*, *115*(8), 1781–1800. https://doi.org/10.1016/j.rse.2011.02.019

Norby, R. J., De Kauwe, M. G., Domingues, T. F., Duursma, R. A., Ellsworth, D. S., Goll, D. S., et al. (2016). Model–data synthesis for the next generation of forest free-air CO2 enrichment (FACE) experiments. *New Phytologist*, *209*(1), 17–28. https://doi.org/10.1111/nph.13593

Ottmar, R. D., Burns, M. F., Hall, J. N., & Hanson, A. D. (1993). *CONSUME: users guide.* (No. PNW-GTR-304). Portland, OR: U.S. Department of Agriculture, Forest Service, Pacific Northwest Research Station. https://doi.org/10.2737/PNW-GTR-304

Pausas, J. G., & Paula, S. (2012). Fuel shapes the fire-climate relationship: evidence from Mediterranean ecosystems: Fuel shapes the fire-climate relationship. *Global Ecology and Biogeography*, *21*(11), 1074–1082. https://doi.org/10.1111/j.1466-8238.2012.00769.x

Pendergrass, A. G., Knutti, R., Lehner, F., Deser, C., & Sanderson, B. M. (2017). Precipitation variability increases in a warmer climate. *Scientific Reports*, *7*(1). https://doi.org/10.1038/s41598-017-17966-y

Polade, S. D., Gershunov, A., Cayan, D. R., Dettinger, M. D., & Pierce, D. W. (2017). Precipitation in a warming world: Assessing projected hydro-climate changes in California and other Mediterranean climate regions. *Scientific Reports*, *7*(1), 10783. https://doi.org/10.1038/s41598-017-11285-y

924 Ren, J., Adam, J. C., Hicke, J. A., Hanan, E. J., Tague, C. L., Liu, M., et al. (2021). How does
925 water yield respond to mountain pine beetle infestation in a semiarid forest? *Hydrology*
926 *and Earth System Sciences*, *25*(9), 4681–4699. https://doi.org/10.5194/hess-25-4681-
927 2021
928 Ren, J., Hanan, E., Abatzoglou, J., Kolden, C., Tague, C., Kennedy, M., Liu, M., Adam, J. (2021
929 a). Code for Projecting future fire regimes in semiarid systems of inland northwestern
930 U.S.: interactions among climate change, vegetation productivity, and fuel dynamics
931 [code]. https://doi.org/10.5281/zenodo.5594757
932 Ren, J., Hanan, E., Abatzoglou, J., Kolden, C., Tague, C., Kennedy, M., Liu, M., Adam, J. (2021
933 b). Data for Projecting future fire regimes in semiarid systems of inland northwestern
934 U.S.: interactions among climate change, vegetation productivity, and fuel dynamics
935 [data set]. https://doi.org/10.17605/OSF.IO/AX45N
936 Rollins, M. G. (2009). LANDFIRE: a nationally consistent vegetation, wildland fire, and fuel
937 assessment. *International Journal of Wildland Fire*, *18*(3), 235–249.
938 Rollins, Matthew G. (2009). LANDFIRE: a nationally consistent vegetation, wildland fire, and
939 fuel assessment. *International Journal of Wildland Fire*, *18*(3), 235–249.
940 https://doi.org/10.1071/WF08088
941 Running, S. W., & Coughlan, J. C. (1988). A general model of forest ecosystem processes for
942 regional applications I. Hydrologic balance, canopy gas exchange and primary production
943 processes. *Ecological Modelling*, *42*(2), 125–154. https://doi.org/10.1016/0304-
944 3800(88)90112-3

945 Schwalm, C. R., Glendon, S., & Duffy, P. B. (2020). RCP8.5 tracks cumulative CO2 emissions.
946 *Proceedings of the National Academy of Sciences*, *117*(33), 19656–19657.
947 https://doi.org/10.1073/pnas.2007117117
948 Simmons, A., & Gibson, J. (2000). The ERA-40 Project Plan.
949 Skinner, K. D. (2013). *Post-fire debris-flow hazard assessment of the area burned by the 2013*
950 *Beaver Creek Fire near Hailey, central Idaho* (USGS Numbered Series No. 2013–1273).
951 Reston, VA: U.S. Geological Survey. Retrieved from
952 http://pubs.er.usgs.gov/publication/ofr20131273
953 Smith, A. M. S., Kolden, C. A., Paveglio, T. B., Cochrane, M. A., Bowman, D. M., Moritz, M.
954 A., et al. (2016). The Science of Firescapes: Achieving Fire-Resilient Communities.
955 *BioScience*, *66*(2), 130–146. https://doi.org/10.1093/biosci/biv182
956 Smith, R. O. (1960). *Geohydrologic evaluation of streamflow records in the Big Wood River*
957 *basin, Idaho* (USGS Numbered Series No. 1479). Washington, D.C.: U.S. Govt. Print.
958 Off.,. Retrieved from http://pubs.er.usgs.gov/publication/wsp1479
959 Son, K., & Tague, C. (2019). Hydrologic responses to climate warming for a snow-dominated
960 watershed and a transient snow watershed in the California Sierra. *Ecohydrology*, *12*(1),
961 e2053. https://doi.org/10.1002/eco.2053
962 Sullivan, M. J. P., Lewis, S. L., Affum-Baffoe, K., Castilho, C., Costa, F., Sanchez, A. C., et al.
963 (2020). Long-term thermal sensitivity of Earth's tropical forests. *Science*, *368*(6493),
964 869–874. https://doi.org/10.1126/science.aaw7578
965 Swann, A. L. S., Hoffman, F. M., Koven, C. D., & Randerson, J. T. (2016). Plant responses to
966 increasing CO2 reduce estimates of climate impacts on drought severity. *Proceedings of*

967 *the National Academy of Sciences*, *113*(36), 10019–10024.
968 https://doi.org/10.1073/pnas.1604581113
969 Tague, C., Seaby, L., & Hope, A. (2009). Modeling the eco-hydrologic response of a
970 Mediterranean type ecosystem to the combined impacts of projected climate change and
971 altered fire frequencies. *Climatic Change*, *93*(1–2), 137–155.
972 https://doi.org/10.1007/s10584-008-9497-7
973 Tague, C. L., & Band, L. E. (2004). RHESSys: Regional Hydro-Ecologic Simulation System—
974 An Object-Oriented Approach to Spatially Distributed Modeling of Carbon, Water, and
975 Nutrient Cycling. *Earth Interactions*, *8*(19), 1–42. https://doi.org/10.1175/1087-
976 3562(2004)8<1:RRHSSO>2.0.CO;2
977 Tang, J., & Riley, W. J. (2020). Linear two-pool models are insufficient to infer soil organic
978 matter decomposition temperature sensitivity from incubations. *Biogeochemistry*, *149*(3),
979 251–261. https://doi.org/10.1007/s10533-020-00678-3
980 Taylor, K. E., Stouffer, R. J., & Meehl, G. A. (2012). An Overview of CMIP5 and the
981 Experiment Design. *Bulletin of the American Meteorological Society*, *93*(4), 485–498.
982 https://doi.org/10.1175/BAMS-D-11-00094.1
983 Thornton, P. E. (1998). Regional ecosystem simulation: Combining surface- and satellite-based
984 observations to study linkages between terrestrial energy and mass budgets, 295.
985 USGS NED. (2016). The National Map. Retrieved from https://www.usgs.gov/core-science-
986 systems/ngp/3dep
987 Warren, J. M., Norby, R. J., & Wullschleger, S. D. (2011). Elevated CO2 enhances leaf
988 senescence during extreme drought in a temperate forest. *Tree Physiology*, *31*(2), 117–
989 130. https://doi.org/10.1093/treephys/tpr002

990 Werf, G. R. van der, Randerson, J. T., Giglio, L., Gobron, N., & Dolman, A. J. (2008). Climate
991 controls on the variability of fires in the tropics and subtropics. *Global Biogeochemical*
992 *Cycles*, *22*(3). https://doi.org/10.1029/2007GB003122
993 Westerling, Anthony L., Turner, M. G., Smithwick, E. A. H., Romme, W. H., & Ryan, M. G.
994 (2011). Continued warming could transform Greater Yellowstone fire regimes by mid-
995 21st century. *Proceedings of the National Academy of Sciences*, *108*(32), 13165–13170.
996 https://doi.org/10.1073/pnas.1110199108
997 Westerling, Anthony LeRoy. (2016). Increasing western US forest wildfire activity: sensitivity to
998 changes in the timing of spring. *Philosophical Transactions of the Royal Society B:*
999 *Biological Sciences*, *371*(1696), 20150178. https://doi.org/10.1098/rstb.2015.0178
1000 Williams, A. P., Abatzoglou, J. T., Gershunov, A., Guzman-Morales, J., Bishop, D. A., Balch, J.
1001 K., & Lettenmaier, D. P. (2019). Observed Impacts of Anthropogenic Climate Change on
1002 Wildfire in California. *Earth's Future*, *7*(8), 892–910.
1003 https://doi.org/10.1029/2019EF001210
1004
1005

[Earth's Future]

Supporting Information for

Projecting future fire regimes in semiarid systems of inland northwestern U.S.: interactions among climate change, vegetation productivity, and fuel dynamics

[1,2]Jianning Ren, [2]Erin J. Hanan, [3]John T. Abatzoglou, [3]Crystal A. Kolden, [4]Christina (Naomi) L. Tague, [5]Maureen C. Kennedy, [1]Mingliang Liu, [1]Jennifer C. Adam

1 Department of Civil & Environmental Engineering, Washington State University, 99163, Pullman, USA

2 Department of Natural Resources and Environmental Sciences, University of Nevada, Reno, 89501, Reno, USA

3 Management of Complex Systems, University of California, Merced, 95344, Merced, USA

4 Bren School of Environmental Science & Management, University of California, Santa Barbara, 93106, Santa Barbara, USA

5School of Interdisciplinary Arts and Sciences, Division of Sciences and Mathematics, University of Washington, Tacoma, 98402, Tacoma, USA

Contents of this file

Introduction

The first part of supplementary material includes a detailed description of WMFire and fire effect model. The second part includes results of RHESSys model calibration and WMFire validation. The third part are supplementary figures to support results and discussion.

Text S1. Model descriptions

S1.1 Fire spread model

WMFire is a stochastic fire-spread model designed to be coupled with RHESSys (Kennedy et al., 2017). It takes output variables from RHESSys and uses them to predict fire spread. Because it is an intermediate-complexity stochastic model, WMFire is not designed to predict the perimeters and timing of individual fires. Instead, the model can be used to predict aggregate spatial and temporal characteristics of fire spread across basins over time (i.e., the fire regime). A successful ignition occurs when there is an ignition source on the landscape, and it successfully starts a wildfire. The successful start of fire (Pi(l,d), Eqn 1) is calculated from the probabilities associate with litter load and relative deficit (Pi(l)) and Pi(d), respectively), where deficit is calculated as 1-ET/PET (here, we use relative deficit as a surrogate for fuel aridity). The probability of a successful spread (Ps(l,d,S,w)) is calculated based on the probabilities associate with litter load (l), relative deficit (d), topographic slope (S) and the orientation of spread relative to wind direction (W), giving Ps(l), Ps(d), Ps(S), and Ps(w), respectively (Eqn 2). The probability of spread (Ps) increases with increasing fuel load and relative deficit, is highest in the direction of wind, increases in the uphill direction, and decreases in the downhill direction. After a successful ignition, WMFire tests the orthogonal neighbors of that patch against the probability of spread to determine if there is a successful spread. WMFire model has demonstrated accuracy in the Santa Fe (New Mexico) and HJ Andrews (Oregon) watersheds (Kennedy et al., 2017).

$$Pi\,(l,d)=Pi\,(l)\times Pi\,(d) \qquad \text{Equation (S1)}$$

$$Ps\,(l,d,S,w)=Ps\,(l)\times Ps\,(d)\times Ps\,(w)\times Ps\,(S) \qquad \text{Equation (S2)}$$

S1.2 Fire effects model

The fire effects model is built to match the complexity of the coupled RHESSys-WMFire model (Bart et al., 2020). The fire effects model uses the probability of spread (Ps) as an index of fire intensity but also accounts for canopy structure, which links fire intensity and spread with fire severity. Fire consumes C in the litter and coarse woody debris (CWD) pools based on the CONSUME model (an empirical model developed using statistical relationships derived from measured woody fuel consumption data; Ottmar et al., 1993). Passive crown fire is spread from the understory to the overstory. For the understory, Ps is a proxy for fire intensity, and the fire-caused mortality is a function of intensity (currently it is a 1:1 linear relationship, but can be changed to account for different landscapes). For the overstory, mortality and consumption of fuel are based on how much litter and understory fuel are consumed. There is also a set of parameters to account for the understory height threshold, overstory height threshold, and functional form representing the relationship between mortality and consumption. The fuel that is not consumed moves into the litter and CWD pools.

Text S2. Model parameterization

We used a Monte Carlo approach to calibrate six groundwater-related parameters: saturated hydraulic conductivity (Ksat), decay of Ksat with depth (m), air-entry pressure (ϕae), pore size index (b), bypass flow to deeper groundwater stores (gw1) and groundwater drainage rates to the stream (gw2). We selected the best parameter set for Trail Creek by comparing observed and modeled streamflow using the Nash-Sutcliffe efficiency metric (NSE), R2 for the correlation between daily observed and modeled flow, and percent error in annual flow estimates as well MODIS ET and NPP (Mu et al., 2011). The Monthly NSE is 0.94 with a percent

error of 2.6 for calibration period. The model estimates ET and NPP in a reasonable range. A detailed description of hydrologic calibration is described by Ren et al., (2021).

The fire spread model WMFire has previously been shown to replicate expected spatial patterns of fire spread for a wildfire in the Pacific Northwest (Kennedy et al., 2017) and fire regime characteristics for two different watersheds with contrasting historical fire regimes (LANDFIRE, Rollins, 2009). The model is robust to applications in both historically low severity frequent-fire regimes in the southwest and mixed to high severity infrequent fire regimes in the Pacific Northwest. We selected three criteria (spatial distribution of fire spread, fire seasonality, fire return interval (FRI) to validate the fire spread model against LANDFIRE estimates for Trail Creek. Spatial distribution and seasonality of fire were not sensitive to ignition rates and agreed with LANDFIRE estimates. FRI, on the other hand, was sensitive to ignition rates. We adjusted ignition rates according to the size of Trail Creek, which enabled RHESSys-WMFire to simulate spatial variation in FRIs that agreed with LANDFIRE estimates. A detailed description of WMFire model calibration is described in (Hanan et al., 2021).

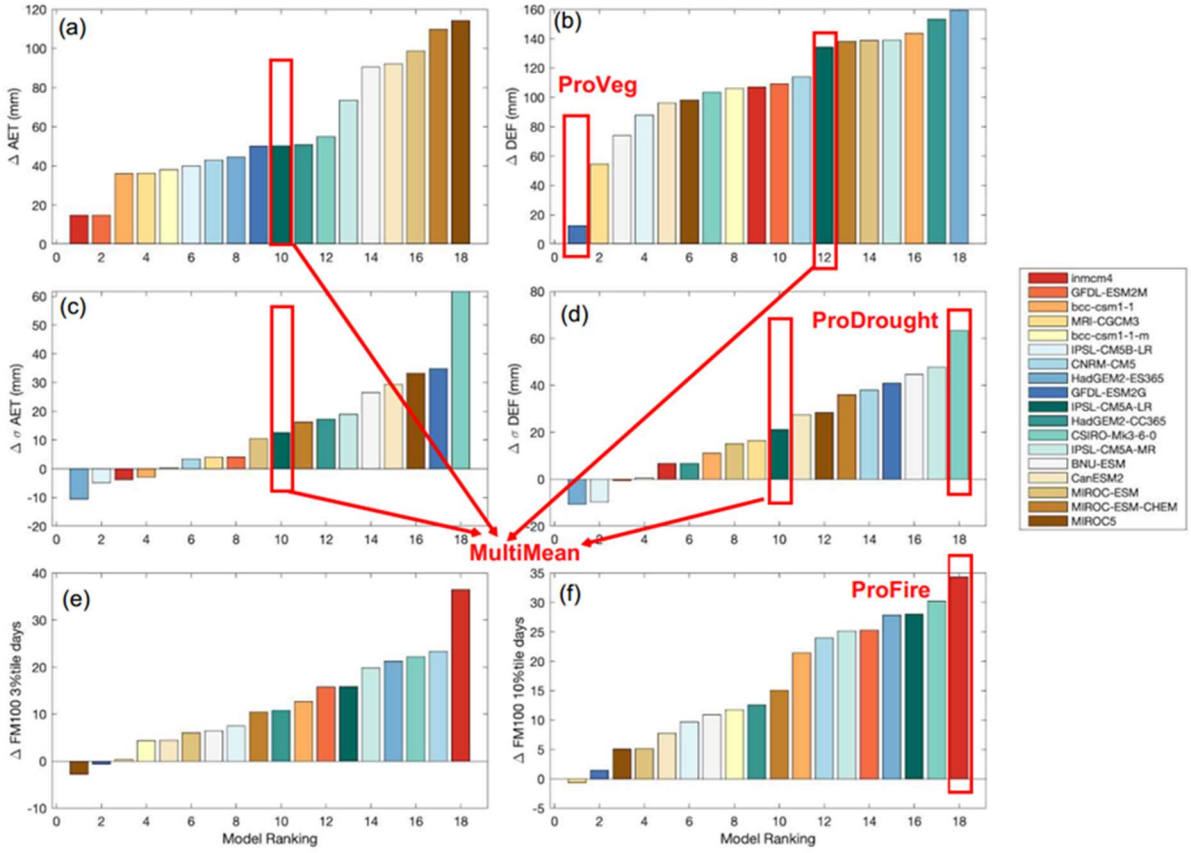

Figure S1. The ranking of fire-related climate change variables among GCM models for Trail Creek according to the future greenhouse gas emission RCP8.5 scenarios. These variables include the 1971 – 2000 vs. 2040 – 2069 changes in the monthly mean of a) actual evaporation (ΔAET) and b) water deficit (ΔDEF), the standard deviation of monthly c) AET (σAET) and d) DEF (σDEF); annual number of days per year where 100-hour dead fuel moisture is below the historical (1971 – 2000) value for the e) 3rd percentile and f) 10th percentile. ProDrought had the

largest increase in the standard deviation of DEF from the historical (1971 – 2000) period; this represents a storyline where drought would be promoted. ProVeg had the smallest increase in the mean of DEF, which would increase productivity and limit fire; and ProFire had significant variability in fire-related metrics; MultiMean is the GCM model that was closest to the multi-model mean.

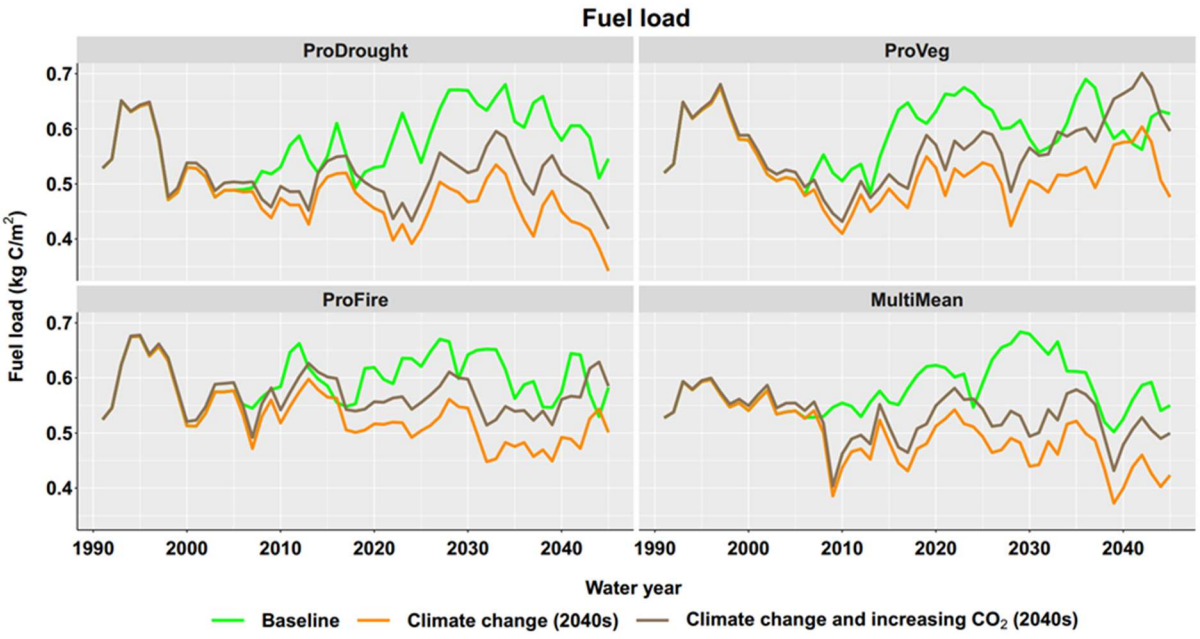

Figure S2. Basin scale fuel load (i.e., litter carbon) response to climate change and atmospheric CO2 fertilization effect under four different GCMs scenarios for 2040s. Baseline scenario used historical climate data for the future scenario spin-up. These scenarios are without fire model on.

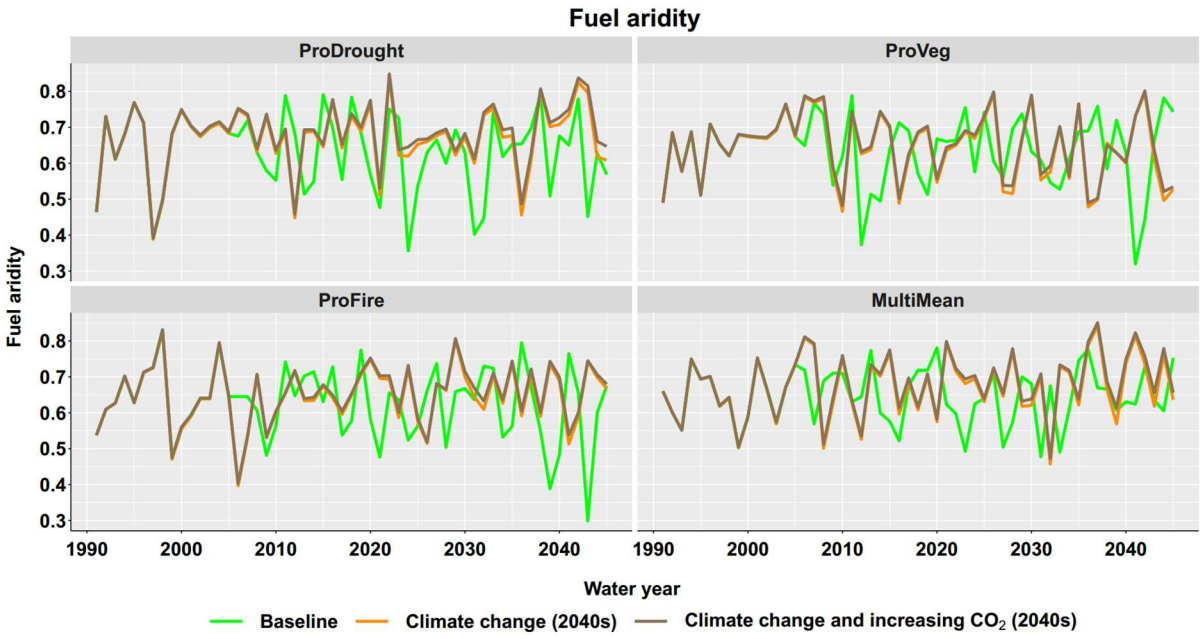

Figure S3. Basin scale fuel aridity response to climate change and atmospheric CO2 fertilization effect under four different GCMs scenarios for 2040s. These scenarios are without fire model on.

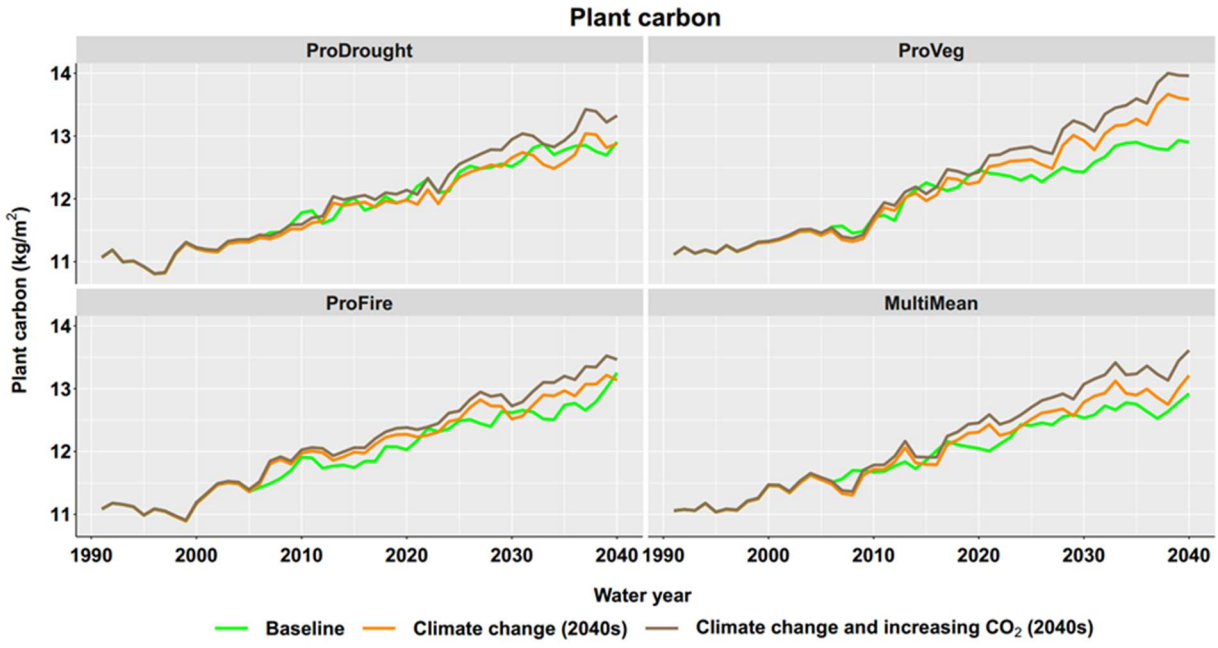

Figure S4. Basin scale plant carbon response to climate change and atmospheric CO2 fertilization effect under four different GCMs scenarios for 2040s. These scenarios are without fire model on.

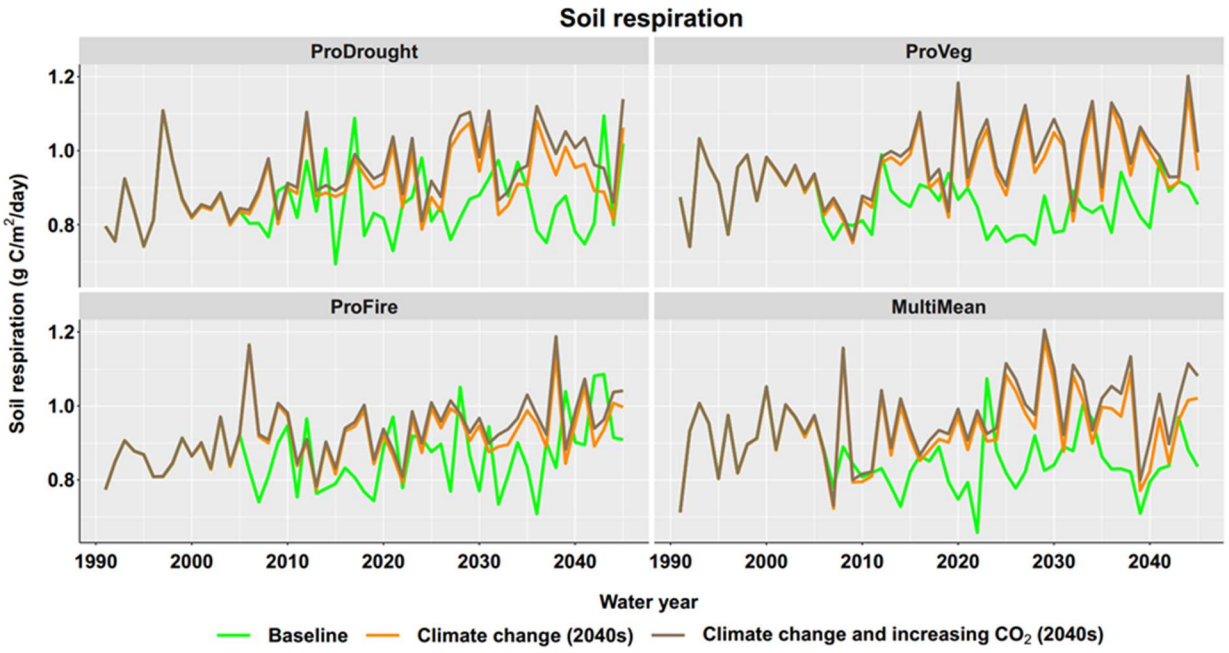

Figure S5. Basin scale soil respiration response to climate change and atmospheric CO2 fertilization effect under four different GCMs scenarios for 2040s. These scenarios are without fire model on.

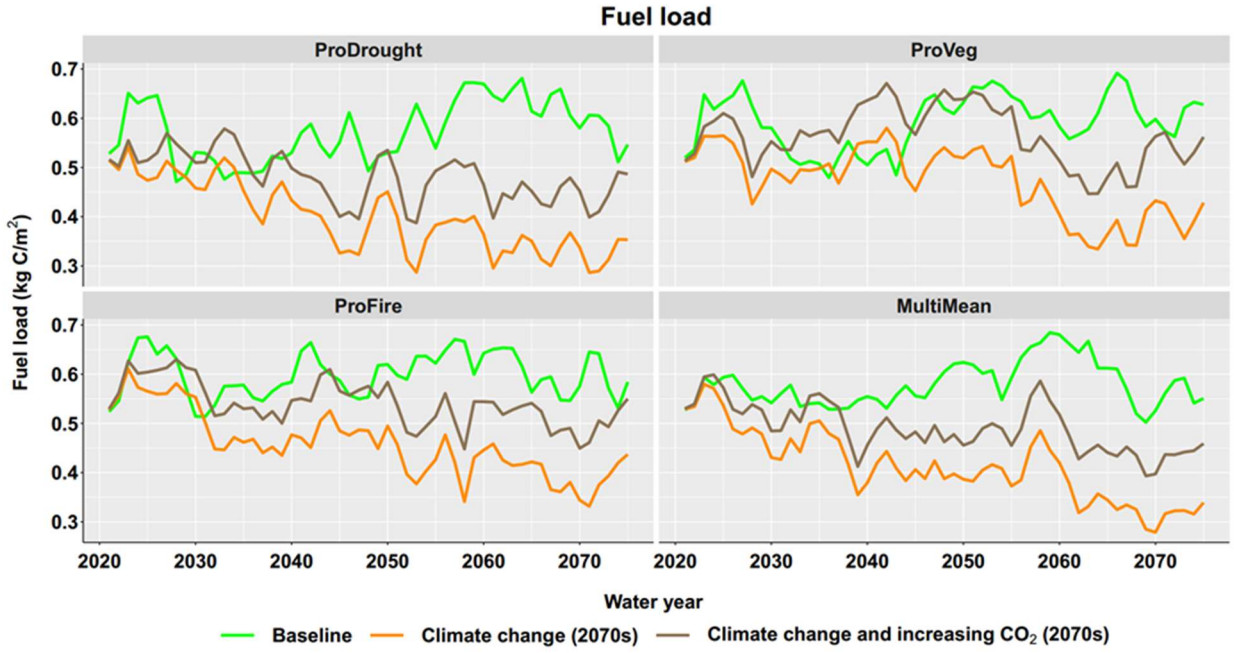

Figure S6. Basin scale fuel load (i.e., litter carbon) response to climate change and atmospheric CO2 fertilization effect under four different GCMs scenarios for 2070s. These scenarios are without fire model on.

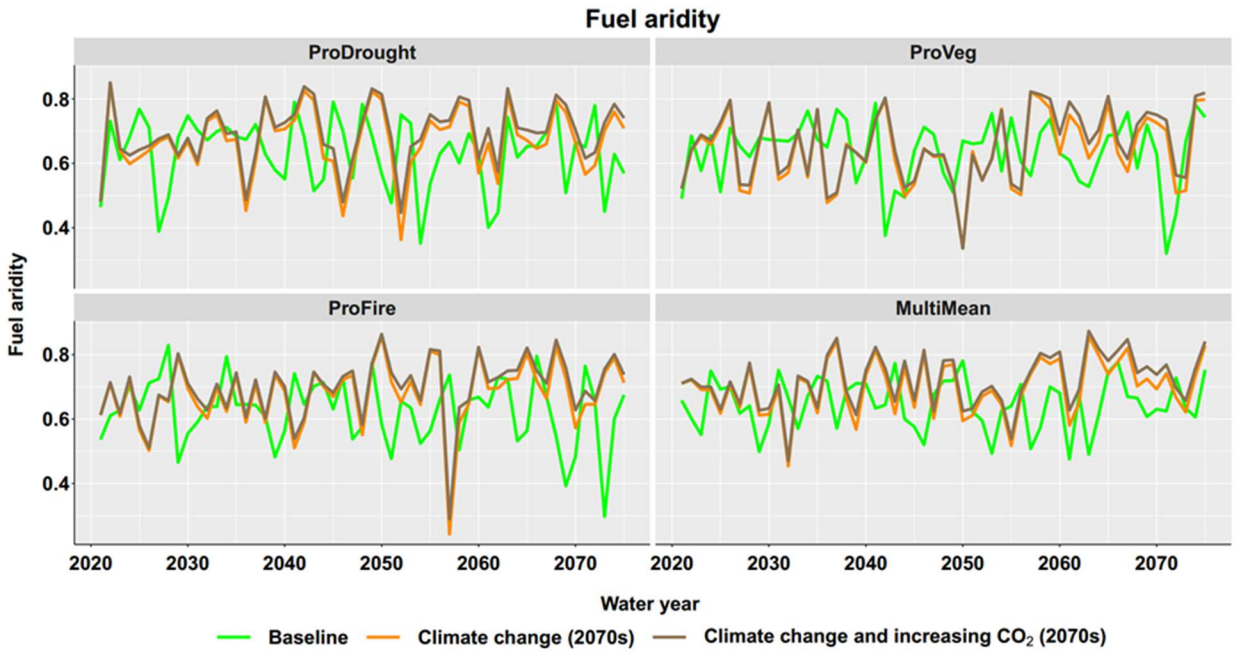

Figure S7. Basin scale fuel aridity response to climate change and atmospheric CO2 fertilization effect under four different GCMs scenarios for 2070s. These scenarios are without fire model on.

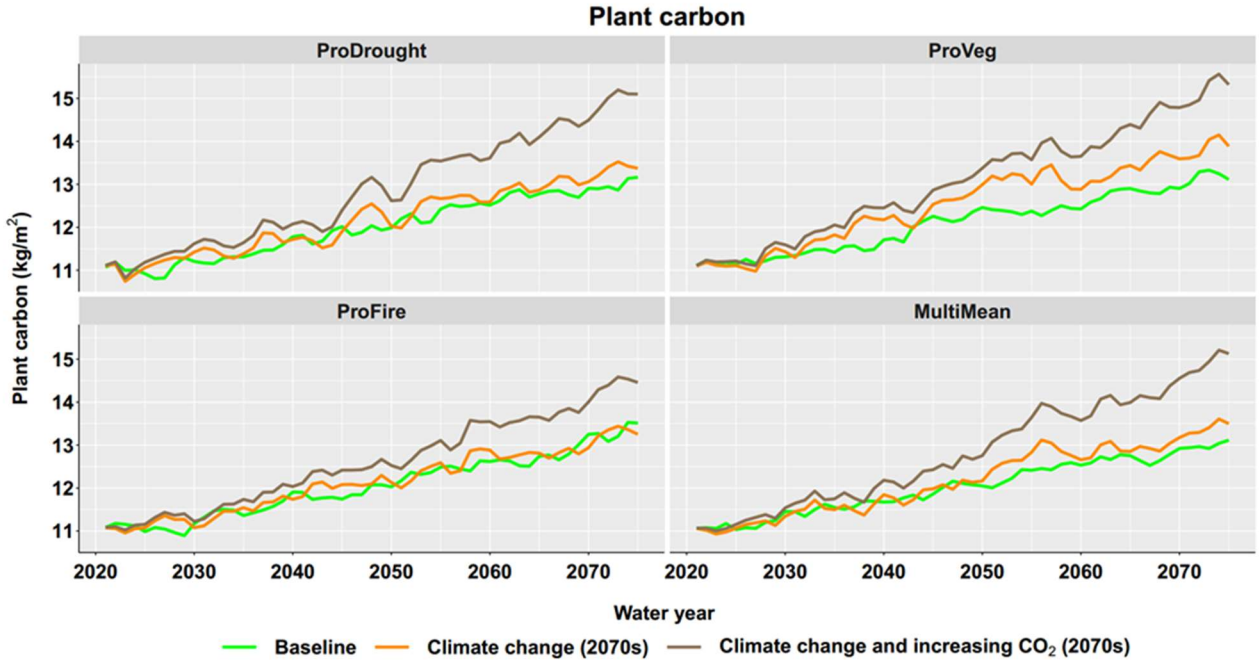

Figure S8. Basin scale plant carbon response to climate change and atmospheric CO2 fertilization effect under four different GCMs scenarios for 2070s. These scenarios are without fire model on.

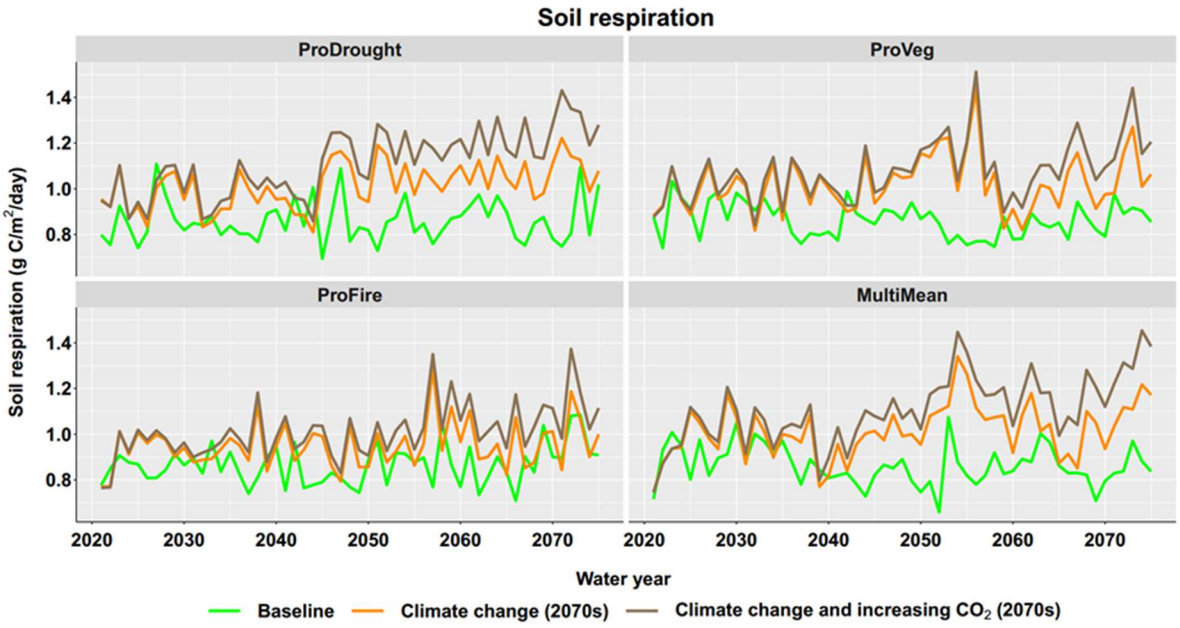

Figure S9. Basin scale soil respiration response to climate change and atmospheric CO2 fertilization effect under four different GCMs scenarios for 2070s. These scenarios are without fire model on.

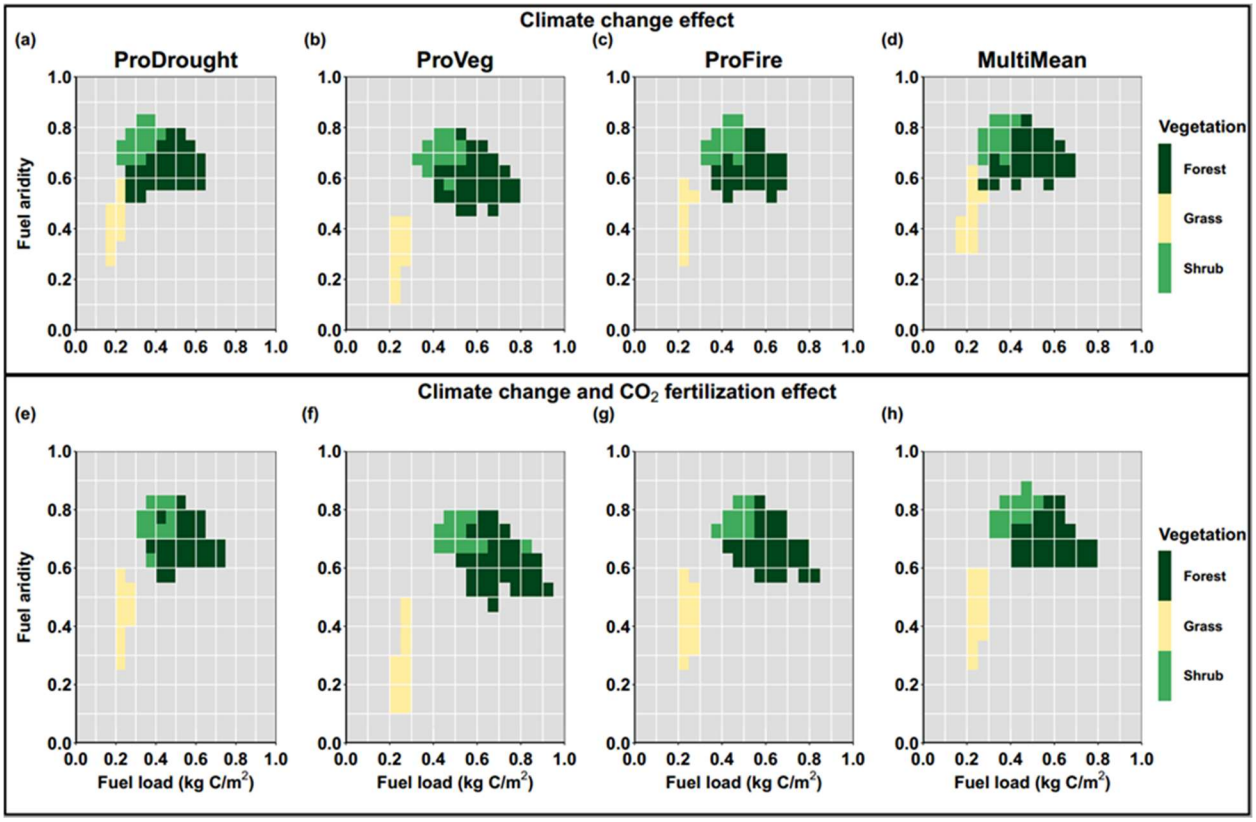

Figure S10. Relationships among fuel load, fuel aridity, and vegetation distribution under various climate change and atmospheric CO2 fertilization effect scenarios in 2040s. Data are bind with 0.05 window length for both fuel load and fuel aridity, and the value of each bin is the median number of vegetation types. Panel (a), (b), (c), and (d) show the only climate change effect and panel (e), (f), (g), and (h) show the overall effect (both climate change and CO2 fertilization effect).

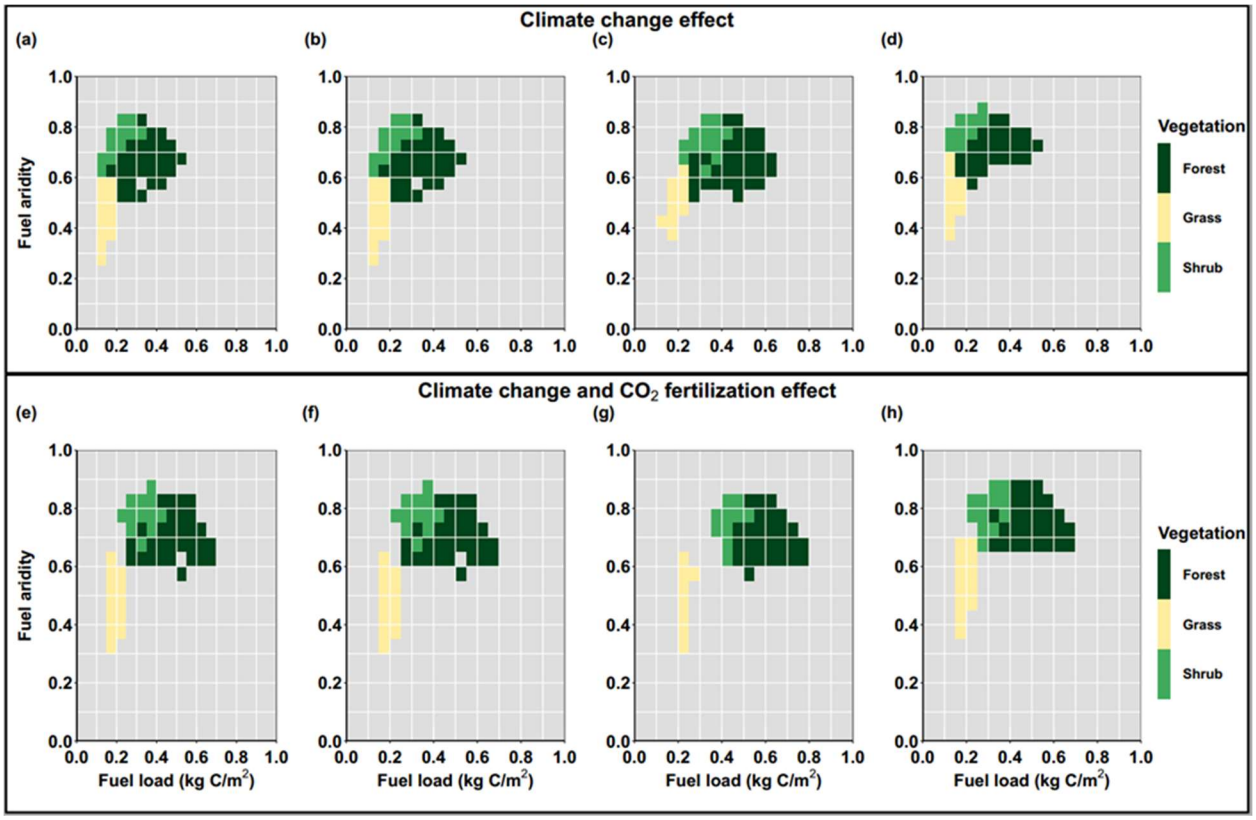

Figure S11. Relationships among fuel load, fuel aridity, and vegetation distribution under various climate change and atmospheric CO2 fertilization effect scenarios in 2070s. Data are bind with 0.05 window length for both fuel load and fuel aridity, and the value of each bin is the median number of vegetation types. Panel (a), (b), (c), and (d) show the only climate change effect and panel (e), (f), (g), and (h) show the overall effect (both climate change and CO2 fertilization effect).

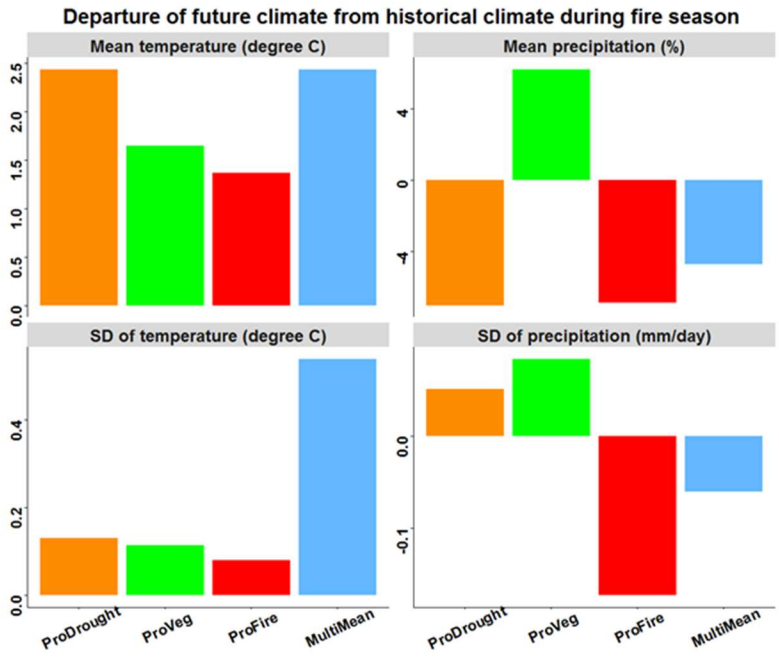

Figure S12. Differences between future climate (2006 - 2060) and historical climate (1991 - 2005) during the fire season (May -September). The top panels are the differences in the annual mean, and the bottom are the differences in the standard deviation (SD).

References:

Bart, R. R., Kennedy, M. C., Tague, C. L., & McKenzie, D. (2020). Integrating fire effects on vegetation carbon cycling within an ecohydrologic model. Ecological Modelling, 416, 108880. https://doi.org/10.1016/j.ecolmodel.2019.108880

Hanan, E. J., Ren, J., Tague, C. L., Kolden, C. A., Abatzoglou, J. T., Bart, R. R., et al. (2021). How climate change and fire exclusion drive wildfire regimes at actionable scales. Environmental Research Letters, 16(2), 024051. https://doi.org/10.1088/1748-9326/abd78e

Kennedy, M. C., McKenzie, D., Tague, C., & Dugger, A. L. (2017). Balancing uncertainty and complexity to incorporate fire spread in an eco-hydrological model. International Journal of Wildland Fire, 26(8), 706. https://doi.org/10.1071/WF16169

Mu, Q., Zhao, M., & Running, S. W. (2011). Improvements to a MODIS global terrestrial evapotranspiration algorithm. Remote Sensing of Environment, 115(8), 1781–1800. https://doi.org/10.1016/j.rse.2011.02.019

Ottmar, R. D., Burns, M. F., Hall, J. N., & Hanson, A. D. (1993). CONSUME: users guide. (No. PNW-GTR-304). Portland, OR: U.S. Department of Agriculture, Forest Service, Pacific Northwest Research Station. https://doi.org/10.2737/PNW-GTR-304

Ren, J., Adam, J. C., Hicke, J. A., Hanan, E. J., Tague, C. L., Liu, M., et al. (2021). How does water yield respond to mountain pine beetle infestation in a semiarid forest? Hydrology and Earth System Sciences, 25(9), 4681–4699. https://doi.org/10.5194/hess-25-4681-2021

Rollins, M. G. (2009). LANDFIRE: a nationally consistent vegetation, wildland fire, and fuel assessment. International Journal of Wildland Fire, 18(3), 235–249. https://doi.org/10.1071/WF08088